

## TOPICAL REVIEW

# Nanoemulsions: formation, structure, and physical properties

T G Mason<sup>1,2,3,4</sup>, J N Wilking<sup>1</sup>, K Meleson<sup>1</sup>, C B Chang<sup>1</sup> and S M Graves<sup>1</sup><sup>1</sup> Department of Chemistry and Biochemistry, University of California—Los Angeles,  
Los Angeles, CA 90095, USA<sup>2</sup> Department of Physics and Astronomy, University of California—Los Angeles, Los Angeles,  
CA 90095, USA<sup>3</sup> California NanoSystems Institute, University of California—Los Angeles, Los Angeles,  
CA 90095, USAE-mail: [mason@chem.ucla.edu](mailto:mason@chem.ucla.edu)

Received 5 July 2006, in final form 18 August 2006

Published 29 September 2006

Online at [stacks.iop.org/JPhysCM/18/R635](http://stacks.iop.org/JPhysCM/18/R635)**Abstract**

We summarize procedures for producing ‘nanoemulsions’ comprised of nanoscale droplets, or ‘nanoemulsions’, methods for controlling the droplet size distribution and composition, and interesting physical properties of nanoemulsions. In contrast to more common microscale emulsions, nanoemulsions exhibit optical transparency at high droplet volume fractions,  $\phi$ , surprisingly strong elasticity at low  $\phi$ , and enhanced diffusive transport and shelf stability. For these reasons, nanoemulsions have great potential in a wide range of industries including pharmaceuticals, foods, and personal care products.

**Contents**

1. Introduction	636
1.1. Overview and organization	636
1.2. Emulsions: dispersions of liquid droplets in another immiscible liquid	636
1.3. Nanoemulsions are not lyotropic liquid crystalline ‘microemulsion’ phases	642
1.4. Nanoemulsions: nanoscale emulsions	643
2. Formation of nanoemulsions	645
3. Manipulating nanoemulsions	651
4. Structure of nanoemulsions	654
5. Physical properties of nanoemulsions	659
6. Nanoemulsion science: frontiers and applications	662
7. Conclusion	663
Acknowledgments	664
References	664

<sup>4</sup> Author to whom any correspondence should be addressed.

## 1. Introduction

### 1.1. Overview and organization

Extreme emulsification methods can be used to produce nanoscale dispersions of droplets of one liquid in another immiscible liquid [1, 2]. These microfluidic and ultrasonic approaches of rupturing larger microscale droplets into nanoscale droplets are providing interesting and useful non-equilibrium systems of structured liquids. Despite their metastability, nanoemulsions can persist over many months or years due to the presence of a stabilizing surfactant that inhibits the coalescence of the droplets [3]. Although one might initially imagine that there are no significant fundamental differences between nanoemulsions and their microscale counterparts, in fact, the physical properties of nanoemulsions can be quite different from those of microscale emulsions, as we demonstrate herein.

Nanoemulsions are part of a broad class of multiphase colloidal dispersions [4]. Although some lyotropic liquid crystalline phases, also known as ‘micellar phases’, ‘mesophases’, and ‘microemulsions’, may appear to be similar to nanoemulsions in composition and nanoscale structure, such phases are actually quite different. Lyotropic liquid crystals are equilibrium structures comprised of liquids and surfactant, such as lamellar sheets, hexagonally packed columns, and wormlike micellar phases, that form spontaneously through thermodynamic self-assembly. By contrast, nanoemulsions do not form spontaneously; an external shear must be applied to rupture larger droplets into smaller ones. Compared to microemulsion phases, relatively little is known about creating and controlling nanoemulsions. This is primarily because extreme shear, well beyond the reach of ordinary mixing devices, must be applied to overcome the effects of surface tension to rupture the droplets into the nanoscale regime [1]. In the world of nanomaterials, nanoemulsions hold great promise as useful dispersions of deformable nanoscale droplets that can have flow properties ranging from liquid to highly solid and optical properties ranging from opaque to nearly transparent. Moreover, it is very likely that nanoemulsions will play an increasingly important role commercially, since they can typically be formulated using significantly less surfactant than is required for nanostructured lyotropic microemulsion phases.

This review article provides the necessary background and key physical concepts that will enable a wide range of interdisciplinary researchers to enter the important field of nanoemulsions. It also remedies deficiencies in the precision of definitions that have been introduced in a recent opinion [5] which approaches the subject of nanoemulsions from a very limited point of view. The remainder of section 1 provides a more thorough introduction to metastable emulsions and contrasts them with lyotropic ‘microemulsion’ phases. In section 2, we review the special requirements for producing nanoscale emulsions using extreme shear, and we contrast this with the production of common microscale emulsions. Manipulating and controlling the composition and size distribution of nanoemulsions is covered in section 3. This is followed by a description of their structure, as probed using scattering and electron microscopy, in section 4. Reducing droplet sizes to the nanoscale leads to some very interesting physical properties, such as optical transparency and unusual elastic behaviour, as we show in section 5. We conclude with an exploration of the frontiers of nanoemulsion science and describe some potential applications in section 6.

### 1.2. Emulsions: dispersions of liquid droplets in another immiscible liquid

Dispersions of solid particles, polymers, and droplets in a viscous liquid represent a very large class of useful and interesting soft materials [4]. Most multiphase dispersions consist of a continuous phase of a viscous liquid comprised of very small molecules typically up to a few

nanometres in size, and also a dispersed phase comprised of a set of larger, yet not macroscopic, discrete structures of a different material. Typically, the sizes of the dispersed structures are not easily visible to the unaided eye. Such structures, which have lengthscales in the range from a few nanometres up to a few microns in size, have been traditionally called ‘colloids’. In most colloidal dispersions, the sizes of the dispersed structures are small enough and the density difference between the continuous and dispersed phase is also small enough that thermal energy can keep the colloids from sedimenting under gravity for extended periods of time. Moreover, at high volume fractions of the dispersed phase,  $\phi$ , dispersions are known to undergo a variety of interesting structural transitions and can even become viscoelastic materials. A variety of mechanisms can be used to stabilize nanoscale colloids. Repulsive interactions between the colloids, due to excluded volume, charge on the particles’ surfaces, or ‘steric’ interactions arising from brush-like coating of polymers on their surfaces, can effectively prevent particles from aggregating together, and the suspension will remain homogeneous. By contrast, if the interactions between the dispersed phase structures are attractive, then aggregation and rapid sedimentation can occur. The structures of the aggregates can range from compact flocs, which maintain an equilibrium exchange with a gas-like phase of single dispersed particles [6], to, for strong attractions, very tenuous fractal gels that are far from equilibrium [7, 8].

Emulsions are dispersions of one liquid phase in another immiscible liquid phase that are made using mechanical shear [9, 10]. Due to differences in attractive interactions between the molecules of the two liquid phases, an interfacial tension,  $\sigma$ , exists between the two liquids everywhere they are in contact [11]. This interfacial tension can be reduced significantly by adding amphiphilic surface-active molecules, or ‘surfactants’, that are highly soluble in at least one of the liquid phases. Surfactants preferentially adsorb at interfaces, since their molecular structures have non-polar hydrocarbon tails that prefer to be in non-polar liquids, such as oils, and polar or charged head groups that prefer to reside in polar liquids, such as water. The energy required to create additional interfacial area,  $A$ , between the two liquids in contact is  $\sigma A$ , so the interfacial tension always acts to minimize the interfacial area between the two liquid phases and keep the interfaces smooth. The interface between two pure immiscible liquid phases forms a planar sheet (figure 1(a)) except at the very edges where the contact angle of the liquids with the solid wall of the container curves the meniscus, which we can neglect for this discussion. The upper liquid phase (e.g. a hydrocarbon oil) has a mass density that is smaller than that of the lower liquid phase (e.g. water). In the absence of any surfactants or other impurities, over a long period of time, the system will always revert to this lowest energy configuration at thermodynamic equilibrium. Even after, if the lyotropic phase is sheared to produce non-equilibrium structures, such as multi-lamellar vesicles [12], these ephemeral structures will coalesce and eventually disappear.

To make a long-lived emulsion of droplets that can persist over weeks or years without coalescing, it is necessary to add a surfactant, which is usually soluble in the continuous liquid phase but not highly soluble in the dispersed phase. This specification of solubility is not a rule without exceptions, but it is generally the case. A system of classification of the tendency of surfactants to disperse in polar or non-polar liquids is referred to as the hydrophile–lipophile balance (HLB) [11], and a numerical HLB scheme exists for classifying surfactants in terms of their relative solubility in aqueous and oily liquid phases.

As an example, in figure 1(b), an anionic surfactant, such as sodium dodecylsulfate (SDS), has been added to the aqueous phase. Due to the charged head group, the surfactant molecules would pay a huge energy cost to enter the non-polar liquid, so their concentration in this liquid is extremely low. Screening cations, such as  $\text{Na}^+$ , although not shown explicitly, are also present in the polar phase to maintain charge neutrality. The surfactant molecules preferentially adsorb to the interfaces, and they maintain an equilibrium surface concentration through a continuous

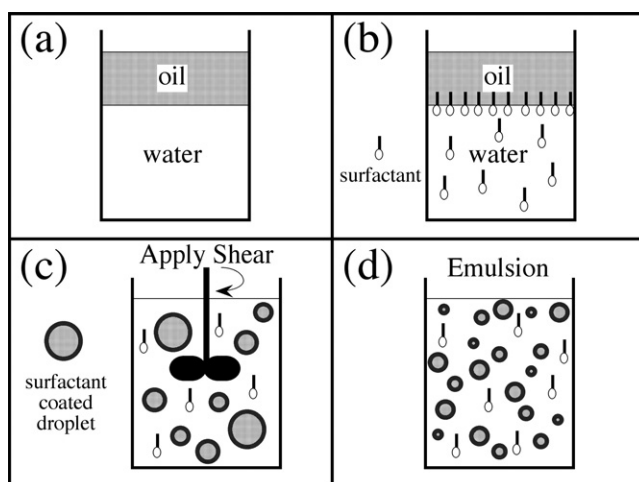


**Figure 1.** (a) Two immiscible liquids, such as oil and water, will phase separate into a layer of the less dense liquid on top of a layer of the more dense liquid below with a flat interface to minimize the interfacial and gravitational energies. (b) A surfactant, generally soluble in the continuous phase, preferentially adsorbs on the oil–water interface and exchanges with monomers and micelles in solution. In this example, the surfactant is soluble in the water phase, so a direct emulsion is anticipated. (c) Shear is applied to the system, causing the oil to break up into droplets that are coated with surfactant and are inhibited from coalescing due to the interfacial repulsion. As the emulsion is sheared, larger oil droplets are stretched, undergo a capillary instability, and rupture into smaller droplets. (d) After the shear has been stopped, the emulsion can persist for many years, and a fraction of the shear energy applied is stored in the greater surface area of the droplets.

dynamic exchange with monomers (and possibly larger assemblies such as surfactant micelles) in the continuous phase. If two oil–water interfaces of droplets coated with surfactant are brought close to one another, then a thin film of water between the interfaces is formed. Due to the like charges of the surfactant, the two interfaces repel each other and the surfactant has stabilized the film against rupturing so the droplets will not coalesce. If one imagines pushing the interfaces to make the film thinner, then eventually it may be possible to exceed a critical disjoining pressure,  $\Pi_d$ , and the film will rupture [13]. For many surfactants, this critical disjoining pressure can be quite large relative to thermal fluctuations and external mechanical perturbations, thereby providing a mechanism for long-term persistence of interfaces without coalescence.

Emulsions are classified not only based on composition, but also based on morphology. Emulsions that have water as a continuous phase and oil as a dispersed phase are called ‘direct’, ‘water-based’, and ‘O/W’ emulsions; for direct emulsions, the surfactant is generally soluble in the aqueous phase and provides more stability of water films. By contrast, emulsions that have oil as a continuous phase are called ‘inverse’, ‘oil-based’, or ‘W/O’ emulsions; for inverse emulsions, the surfactant is generally soluble in the oil phase and provides more stability of oil films. For emulsions, the surfactant does not lower  $\sigma$  to effectively zero; instead the surface tension, although somewhat reduced, remains at a large value, typically  $\sigma \geq 1 \text{ dyn cm}^{-1}$ . At low  $\phi$ , an isolated droplet is spherical and has a radius,  $a$ . The curved interface exerts a pressure on the molecules inside the droplet, and this pressure is called the Laplace pressure [11],  $\Pi_L = 2\sigma/a$ . For non-spherical droplets,  $\Pi_L$  is proportional to the sum of the inverse of the two principal radii of curvature of the interface. Due to the inverse dependence of  $\Pi_L$  on  $a$ , the molecules in smaller droplets experience a higher pressure than those in larger droplets.

There are two primary mechanisms that can destabilize the emulsion and cause the droplet size distribution to change [3]. The first is coalescence, caused by the rupturing of films of the continuous phase and the fusion of two droplets into a single larger droplet. By choosing a surfactant that provides a strong repulsion between droplet interfaces, coarsening through coalescence can also be effectively eliminated even at large  $\phi$ , provided that  $\Pi_d$  is not exceeded. The second mechanism leading to destabilization of the emulsion can occur if molecules of the dispersed phase have a relatively high solubility in the continuous phase. The diffusive migration of individual dispersed phase molecules that are driven from smaller droplets, which have a higher Laplace pressure, to larger droplets, which have a lower Laplace pressure, is known as ‘Ostwald ripening’ [3, 14]. By selecting molecules of the dispersed phase that have very low solubility in the continuous phase, the rates associated with Ostwald ripening can become so low that no changes in droplet sizes can be detected over years [15–17]. Thus, for emulsions, choosing an appropriate composition can essentially eliminate both destabilization mechanisms. By contrast, it is very difficult to eliminate Ostwald ripening in gaseous foams [15, 16] because the gas molecules inside the bubbles dissolve readily in common liquid phases.

Classical ‘metastable emulsions’ [18, 9, 19, 20] are formed by applying mechanical shear to the continuous phase in order to break larger droplets of the dispersed phase into smaller droplets (figure 1(c)). This process is generally called ‘emulsification’. To significantly deform a droplet, the applied shear stress,  $\tau$ , must approach and exceed the Laplace pressure [21]. Thus, in order to stretch and break droplets down to smaller and smaller sizes, it is necessary to apply increasingly large viscous stresses:  $\tau = \eta_c \dot{\gamma}$ , where  $\dot{\gamma}$  is the shear rate and  $\eta_c$  is the viscosity of the continuous liquid phase. Due to the presence of excess surfactant in the bulk continuous phase, as soon as the interfacial area is created by the shear, surfactant coats these interfaces. As the interfaces of large droplets are stretched into elongated ellipses and even threads, they undergo a capillary instability [22] driven by surface tension that leads to rupturing. Unstable to varicose deformations, the elongated droplet necks down and pinches off to form smaller droplets [22, 20]. Although the surfactant typically provides a strong disjoining pressure for films containing the continuous phase, it provides very little resistance against rupturing of films containing the dispersed phase. This asymmetry in the stabilization of the films enables the capillary instability to completely pinch-off droplets of the dispersed phase in the continuous phase without the opposite process occurring.

The fundamental relationship governing how an isolated droplet of one liquid can be ruptured in another immiscible liquid through the application of a shear stress has been developed by Taylor during the last century [18]. In the simplest case where the dispersed phase viscosity,  $\eta_d$ , can be ignored, the typical size of the ruptured droplets is governed by Taylor’s formula [18]:  $a \approx \sigma / (\eta_c \dot{\gamma})$ . We have neglected pre-factors of order unity which depend on many experimental details and also the formation of satellite droplets during capillary-driven breakup. Taylor’s basic relationship captures the essence of emulsification, yet it is just the doorway to a very broad range of work on the capillary instability. It must be modified significantly for isolated droplets (i.e. in the limit  $\phi \rightarrow 0$ ) in a variety of steady and transient flows [23, 20, 24–26, 19, 27, 28]. Inertial effects can also be important in certain regimes [24, 29]. Comparatively less is known about how droplet rupturing occurs for concentrated emulsions at large  $\phi$ , yet some studies have begun to address this issue [30–33, 1]. Non-Newtonian rheological properties of surfactant mesophases and polymeric liquids can strongly affect the capillary instability [31, 34]. Whether the shear is applied to an emulsion having either high or low  $\phi$ , the size distribution of the ruptured droplets is determined by the *history of applied shear*. Merely knowing the composition of the emulsion is not enough to specify its structure and physical properties.

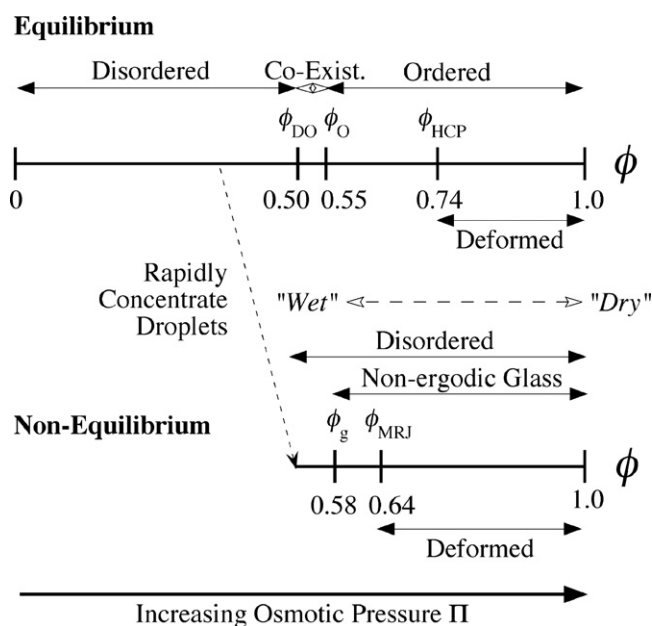


**Figure 2.** Diagram of structural transitions in monodisperse emulsions as a function of droplet volume fraction,  $\phi$ . The upper equilibrium branch shows a disordered liquid-like structure of spherical droplets up to the disorder–order transition  $\phi_{DO} \approx 0.50$ , above which there is a coexistence of ordered and disordered phases until the droplets become completely ordered at  $\phi_O \approx 0.55$ . At larger  $\phi$  up to  $\phi_{HCP} = 0.74$ , associated with random hexagonal close packing (HCP), the spherical droplets remain ordered and undeformed, and thermal energy causes them to fluctuate about their equilibrium configuration. For  $\phi > 0.74$ , the ordered droplets deform as the continuous liquid is removed from between them. The equilibrium branch is difficult to achieve empirically because the droplets must be very uniform in size and must be concentrated very slowly. The lower glassy branch is typical of emulsions that are rapidly concentrated (i.e. quenched) into a disordered structure at larger  $\phi$ . Empirically, at the glass-transition volume fraction,  $\phi_g$ , the droplets become permanently caged by their neighbours, and the emulsion undergoes an ergodic to non-ergodic transition. For  $\phi_g < \phi < \phi_{MRJ}$ , the undeformed spherical droplets can diffuse inside the cages, and they jam together at the maximum random jamming (MRJ) volume fraction  $\phi_{MRJ} = 0.64$  (previously associated with random close packing). Above  $\phi_{MRJ}$ , the disordered droplets deform and change from nearly spherical at the ‘wet’ foam limit to faceted polyhedra towards the ‘dry’ foam limit as  $\phi$  approaches unity.

Following emulsification at high shear rates, a well-designed stable emulsion under quiescent conditions has a well-defined droplet size distribution that does not evolve. Other stresses, such as gravitational, thermal, interfacial, and electrostatic, influence the structure and behaviour of the emulsion. After the shear has been removed, the positional structure of the droplets is typically disordered, and the droplets assume shapes dictated primarily by  $\phi$  and  $\sigma$ . Despite being called ‘metastable’, model emulsions can persist for months, years, and even decades without a significant evolution of the droplet size distribution [17]. In such cases, the term metastable really only refers to how the emulsion has been created and does not imply that the emulsion is coarsening. Although the total surface area of the droplets (see figure 1(d)) is much larger than that of two phase-separated liquids (see figure 1(b)), the probability that thermal energy would overcome  $\Pi_d$  and cause significant droplet coalescence is essentially zero over practical timescales.

Stable emulsions can be concentrated from low  $\phi$  to high  $\phi$  through the application of an osmotic pressure,  $\Pi$  [35, 36] (see figure 2). Consider a model ‘monodisperse’ emulsion of

identical droplets. The microscopic positions and shapes of the droplets, and, consequently, the macroscopic physical properties of the emulsion change as  $\phi$  is increased. For simplicity, we assume that the interactions between the droplets are strongly repulsive only at very short range, thereby creating ‘hard interfacial repulsions’ [4]. Here, the word ‘hard’ is used to refer to the negligible range of the interaction potential, not to the nature of the droplet interfaces, which remain deformable. As the droplets are concentrated, they more frequently encounter their neighbours as they diffuse through Brownian motion. The emulsion’s viscosity,  $\eta$ , increases until the droplet crowding becomes extreme, and  $\eta$  becomes dependent on the shear rate. If the droplets are very slowly concentrated through a ‘quasi-static’ reversible osmotic process (figure 2—upper branch), as  $\phi$  exceeds roughly  $\phi_{\text{DO}} \approx 0.50$ , they undergo a disorder–order transition and begin to crystallize in order to increase the available room for diffusive translational motion [37, 4]. This disorder–order transition is entropic in origin and phase coexistence between disordered and ordered (i.e. crystalline) positional structures persists until  $\phi \approx 0.55$ . Further concentration of the emulsion reduces the translational free volume per droplet [35], but does not alter the structure, other than through small changes in the interdroplet separation. At the volume fraction associated with random hexagonal close packing  $\phi_{\text{HCP}} \approx 0.74$ , the droplets effectively touch and pack, and they begin to deform for larger  $\phi > \phi_{\text{HCP}}$ . Finally, in the so-called ‘dry’ limit,  $\phi \rightarrow 1$  [38–40], the emulsion resembles a network of thin films, interconnected triangular ridges known as plateau borders, and vertices where four plateau borders typically intersect [3, 41]. Such highly concentrated emulsions are also referred to as ‘bilibiquid foams’, since they essentially resemble well-drained gaseous foams of highly deformed bubbles.

By contrast, if the droplets are concentrated very rapidly without causing coalescence, then they maintain a disordered configuration even above  $\phi_{\text{DO}}$  until the droplets form a disordered glass and begin to jam and deform [42–44] (see figure 2—lower branch). Although there is some debate about how this occurs, concentrating the droplets leads to a kinetic arrest at volume fractions around  $\phi_{\text{g}} \approx 0.58$ , known as ‘the glass transition volume fraction’ associated with an ergodic to non-ergodic transition [45–48]. For  $\phi > \phi_{\text{g}}$ , the disordered droplets can neither rearrange nor switch positions with neighbouring droplets, even though they are not jammed. Moving toward larger  $\phi$ , the disordered droplets actually jam and their interfaces effectively ‘touch’ at  $\phi \approx 0.64$ , as revealed by measurements of the osmotic pressure and shear modulus of monodisperse emulsions [35]. Subsequent molecular dynamics simulations have demonstrated the onset of droplet deformation to be at  $\phi = 0.64$ , the first real agreement between a microscopic model of a soft glassy material of deformable spheres and the macroscopic experimental observations without any adjustable parameters [42, 49, 50]. In recent years, this volume fraction has been associated with ‘maximal random jamming’ (MRJ),  $\phi_{\text{MRJ}} \approx 0.64$  [43, 51, 44]. This is a more precise definition of a concept known in earlier years as the volume fraction associated with ‘random close packing’ (RCP),  $\phi_{\text{RCP}} \approx 0.64$  [52, 53]. Once the spherical droplets have jammed, any further increase in  $\phi$  will cause the droplet interfaces to deform. Of course, the meaning of jamming for emulsions is more complex than for hard spheres, since a thin film of liquid must be preserved between the droplets in order to preclude coalescence. Also, jamming transitions are affected by the shapes of the constituent particles or droplets [54]. For disordered monodisperse emulsions, the jamming transition is associated with the onset of significant deformation of the droplets [48, 35]. Such glassy emulsions of jammed droplets can also be concentrated up to volume fractions approaching unity, yielding disordered biliquid foams. The interfacial structure of ‘dry’ foams, whether biliquid or gaseous, has been studied in significant detail through accurate simulations [55–57].

Whether or not the positional structure of the emulsion is ordered or disordered, highly concentrated emulsions having  $\phi > \phi_{\text{MRJ}}$  exhibit an elastic shear response. The overall

magnitude of an emulsion's elastic shear modulus in this regime is determined by the average Laplace pressure, since the shear must do work against the interfacial tension to stretch the compressed droplets. Of course, for the system to remain as an emulsion,  $\phi$  cannot actually reach unity, and, in reality, extreme osmotic pressures can cause droplet coalescence if the osmotic pressure exceeds the critical disjoining pressure. Such extreme osmotic pressures can occur through the evaporation of the continuous phase.

As with other colloidal dispersions, the structure of emulsions can be significantly altered from this picture of hard interfacial contact repulsions by the presence of attractive interactions. Altering the composition of the continuous phase can lead to attractive interactions between droplets. In some cases, the attraction can exist without also causing droplet coalescence. For instance, adding salt (e.g. NaCl) to SDS-stabilized oil-in-water emulsions can create a deep secondary minimum in the interdroplet pair potential, leading to the formation of fractal aggregates and gels of droplets in which the droplets do not coalesce [58]. Despite the attraction, a thin film of the continuous phase still persists, so the droplets form slippery bonds with their neighbours. However, if the composition of the emulsion is altered so that the attractive interaction becomes strong enough that the secondary minimum merges with the primary van der Waals minimum, the films between the droplets can become unstable and coalesce. This scenario typically leads to rapid destabilization of the emulsion and ultimately to phase separation. An interesting example illustrating this is 'viscous sintering' of direct emulsions comprised of highly viscous asphalt droplets that are chemically quenched to eliminate the charge repulsion, fuse together, and gradually contract [59].

### *1.3. Nanoemulsions are not lyotropic liquid crystalline 'microemulsion' phases*

By contrast to metastable nanoemulsions described in the preceding paragraphs, 'microemulsions' represent a complex menagerie of completely different equilibrium systems [60, 11, 61]. So-called 'spontaneous emulsification' through the addition of a surfactant without shear are usually related to the formation of equilibrium lyotropic liquid crystalline phases, in which the surface tension effectively vanishes and the droplets are formed by thermodynamic molecular self-assembly from the 'bottom up' [62]. These lyotropic phases, sometimes referred to as 'microemulsions', 'mesophases', or 'swollen micelles', are *not* emulsions in the classical sense. In most microemulsion phases, the surfactant is highly soluble in both liquid phases, and the two immiscible liquid phases themselves also have relatively high mutual solubility. Microemulsions are true self-assembled thermodynamic phases that can have very interesting morphologies such as planar stacks of lamellae (lamellar phases), hexagonally packed tubes (hexagonal phases), and spherical droplets (spherical micellar phases).

Researchers new to the field of emulsions can easily be confused into thinking that spherical micellar phases are essentially the same as nanoemulsions, since they both have spherical nanoscale 'droplet' structures and the compositions both typically contain oil, water, and surfactant. The two systems are very different since nanoemulsions are formed by mechanical shear and microemulsion phases are formed by self-assembly. Another common mistake is to describe microscale emulsions as 'microemulsions', thereby confusing an emulsion system with a thermodynamic phase. In retrospect, the historical choice of the word 'microemulsion' to describe nanoscale self-assembled phases is unfortunate, since these phases typically have structures between roughly 1 and 100 nm, the same range as for nanoemulsions. 'Microemulsions' are not emulsions of microscale droplets formed by shear, but rather nanoscale self-assembled equilibrium phases in which surface tension does not play a significant role. Although both microemulsions and emulsions can be comprised of three simple components, surfactant, oil, and water, the distinguishing difference between

equilibrium microemulsions and metastable microscale emulsions is not one of composition, but rather one of thermodynamics. Generally, metastable emulsions have a high surface tension between oil and water phases, the relative solubility of the dispersed phase in the continuous phase is very low, and the surfactant is soluble only in the continuous phase.

An approach to making nanoscale droplets using surfactant mixtures and varying the temperature relative to the phase inversion temperature (PIT) to convert bicontinuous microemulsion phases [63] into nanoscale droplets without extreme shear has been discussed in a recent opinion entitled 'Nano-emulsions' [5]. The authors of the opinion claim that such an approach can be used to form metastable nanoemulsions. This claim is not appropriate because it ignores the thermodynamic distinctions between nanoemulsions and microemulsions. It is inappropriate to have the word nanoemulsion in a ternary phase diagram that also contains the word microemulsion. The authors' choice of terminology incorrectly implies that a lyotropic liquid crystalline phase can be converted into a nanoemulsion just by varying the temperature to achieve a reduction of the surface tension into the range from  $10^{-2}$  to  $10^{-5}$  dyn cm<sup>-1</sup> without applying shear. Systems having such low surface tensions are basically microemulsion phases according to the original conventional definition [60], and they will convert back into other types of microemulsion phases if the system is returned to its original starting temperature. Nanoemulsions do not have such minute surface tensions, and they will not convert into other types of microemulsion phases when the temperature is varied. Nanoemulsions are formed when larger droplets are ruptured into smaller ones using extreme shear to overcome a large surface tension [1]. The large surface tension prevents lyotropic self-assembly from playing any role in the emulsification process. Indeed, a very recent review of self-emulsification indicates that nanoscale droplets created using PIT procedures have a lamellar layer on their surfaces and do not remain stable over long periods of time [61].

Much is already known about emulsions, yet emulsion science still has many frontiers. Books [9], review articles [10, 21], and encyclopedia chapters [3, 17] cover the basic principles of emulsions, so only the most relevant aspects related to this specific review on nanoemulsions have been briefly described here. Since the structure and physical properties of foam are essentially governed by the same interfacial laws, dispersions of gas bubbles in a continuous liquid phase share many similarities with emulsions. It is also worthwhile developing an understanding of these closely related systems [64, 65, 57, 56, 55, 16, 15].

#### *1.4. Nanoemulsions: nanoscale emulsions*

Simply put, nanoemulsions are dispersions of nanoscale droplets formed by shear-induced rupturing. The present convention for nanoscale materials are materials comprised of structures having lengthscales in the range from 1 to 100 nm; well below this range lies the angstrom scale, and well above this range lies the micro scale. Applying this convention to metastable emulsions, we have defined nanoemulsions to be emulsions having droplet sizes in this 'nano' range. To be more precise about size, one must specify the droplet radius or diameter; in general, we apply the more flexible definition of a nanoemulsion in which the vast majority of droplets both on a number- and volume-weighted basis have radii below 100 nm. Since the diameter and radius only differ by a factor of two, this is a small distinction relative to the two decades of 'nano' lengthscales. Although we have extended the definition of nanoemulsions to the 1 nm scale, it would be impossible to make a nanoemulsion smaller than the size of a surfactant micelle, typically a few nanometres.

Some years ago, the emulsion community adopted the word 'mini-emulsion' to refer to emulsions comprised of submicron droplets [66–69, 2]. Thus, nanoemulsions represent the extreme lower limit of mini-emulsions. In contrast to nanoemulsions, most mini-emulsions are

comprised of droplets in the size range from 100 nm to 1  $\mu\text{m}$ . Although some miniemulsion systems have extended into the size range of nanoemulsions, there is relatively little information about their physical properties. This is largely due to the relative difficulty of making nanoemulsions compared to microscale emulsions and also to the complexity of the methods required to reliably measure the structures of liquid nanoscale systems. Optical microscopy, even using differential interference contrast or other phase contrast methods, is generally not a viable method for examining nanoemulsions. As we will discuss below, more sophisticated techniques, such as dynamic light scattering [70], x-ray or neutron scattering [71], atomic force microscopy, or cryo-electron microscopy [72] are typically required to explore the structure and behaviour of nanoemulsions.

Nanoemulsions can be characterized by specifying molecular constituents, quantities of these constituents, and the sizes of the droplet structures following the formation of the emulsion by shear. For the following discussion, we consider direct nanoemulsions of oil droplets in water; the basic ideas also apply to inverse nanoemulsions. The molecular weight,  $M_w$ , and molecular structure of the oil (e.g. alkane, silicone, or other) are typically chosen based on the application, yet  $M_w$  must be large enough to inhibit Ostwald ripening. The surfactant type and concentration,  $C$ , in the aqueous phase are chosen to provide good stability against coalescence. The droplet volume fraction,  $\phi$ , describes the relative degree of concentration of the droplets. Finally, the droplet structure is typically reported in terms of a size distribution of droplets, commonly measured using dynamic light scattering (DLS) [70] from a diluted sample that has been filtered to remove dust. After data collection, most DLS systems generally employ a regularization algorithm to fit decays in the intensity autocorrelation function to obtain the size distribution,  $p(a)$ . Regularized fitting is ill-posed mathematically, so it is a good idea to compare unknown size distributions with control experiments using calibrated polymer spheres. It is also important to know how the size distribution is weighted; a number-weighted distribution is different from a volume-weighted distribution. Most commercial DLS systems report volume-weighted distributions.

Despite its limitations, DLS can generally be used to provide a volume-weighted mean,  $\langle a \rangle$ , and standard deviation,  $\delta a$ , of the radial size distribution of the droplets. Reliably defining higher moments of the distribution, such as skewness, is typically more difficult to achieve reliably. The polydispersity of the size distribution is typically defined as  $\delta a / \langle a \rangle$ , and distributions are generally referred to as ‘monodisperse’ if  $\delta a / \langle a \rangle < 0.2$ . Although DLS can provide the size distribution, this alone does not determine the droplet positional structure, which can be only determined through neutron or x-ray scattering methods of the liquid emulsions or through electron microscopy techniques, including cryo-transmission electron microscopy (cryo-TEM) and cryo-fracture scanning electron microscopy (cryo-fracture SEM) [72]. Although cryo-EM methods can provide appealing static real space images of droplets at very high magnifications, droplet dynamics cannot be studied, since the emulsions are typically vitrified into a glassy solid phase by quenching the emulsion to a temperature far below room temperature.

Nanoemulsions have some interesting physical properties that distinguish them from ordinary microscale emulsions. For instance, microscale emulsions typically exhibit strong multiple scattering of visible light, and, as a result, have a white appearance. The multiple scattering occurs as the light is refracted many times through droplets, films, and plateau borders, provided there is a significant refractive index contrast,  $\Delta n$ , between the dispersed and continuous phases. In the absence of optical absorption, photons that enter the emulsion are scattered many times by microscale structures before they leave the emulsion. By contrast, the structures in nanoemulsions are much smaller than visible wavelengths, so most nanoemulsions appear optically transparent, even at large  $\phi$  and for large  $\Delta n$ . Table 1 compares several

**Table 1.** Physical characteristics of emulsion droplets. Nanoemulsions (bold type) and microscale emulsions (normal type). We assume direct nanoemulsions having surface tension of  $\sigma = 10 \text{ dyn cm}^{-1}$  and continuous liquid viscosity of  $\eta_c = 1 \text{ cP}$  at room temperature  $T = 298 \text{ K}$ .

Radius $a$ (nm)	Volume $V$ (l)	Laplace pressure $\Pi_L = 2\sigma/a$ (atm)	Shear rate to rupture $\dot{\gamma} \approx \sigma/(a\eta_c)$ ( $\text{s}^{-1}$ )	Thermal energy scale $k_B T/V$ ( $\text{dyn cm}^{-2}$ )
<b>10</b>	<b><math>4 \times 10^{-21}</math></b>	<b>20</b>	<b><math>10^9</math></b>	<b><math>10^4</math></b>
<b>100</b>	<b><math>4 \times 10^{-18}</math></b>	<b>2</b>	<b><math>10^8</math></b>	<b><math>10^1</math></b>
1 000	$4 \times 10^{-15}$	0.2	$10^7$	$10^{-2}$
10 000	$4 \times 10^{-12}$	0.02	$10^6$	$10^{-5}$

other physical properties of nanoemulsions to ordinary emulsions. Nanoemulsions have a much larger surface area to volume ratio than ordinary emulsions, so phenomena related to deformation of the droplets, such as the Laplace pressure and the elastic modulus, are typically larger for nanoemulsions than ordinary emulsions. The number of molecules of the dispersed phase in nanoemulsion droplets are much smaller than for ordinary emulsions and are typically several hundred to many thousand, depending upon  $M_w$ . Common inkjet technology uses picolitre ( $10^{-12}$  l) droplets having radii of several microns. By contrast, nanoemulsions that have a 10 nm radius contain of the order of a zeptolitre ( $10^{-21}$  l) of the dispersed phase. Thus, one single picolitre droplet could be ruptured into a billion nanoemulsion droplets!

## 2. Formation of nanoemulsions

To make a stable emulsion reproducibly, a large number of factors must be controlled. These include selecting an appropriate composition, controlling the order of addition of the components, and applying the shear in a manner that effectively ruptures droplets. There are several additional requirements for nanoemulsions. The dispersed phase molecules must be essentially insoluble in the continuous phase so that Ostwald ripening does not occur rapidly despite the very high Laplace pressures. Suppressing Ostwald ripening can be achieved by other means [73], but choosing a very insoluble liquid for the dispersed phase is the easiest method. The second requirement is a choice of components, especially surfactant, which do not result in the formation of lyotropic liquid crystalline ‘microemulsion’ phases. Systems containing short chain alkanes, alcohols, water, and surfactants are known to form these phases [63]. The third requirement is that the continuous phase has a significant excess of surfactant. This excess enables new surface area of the nanoscale droplets to be rapidly coated during emulsification, thereby inhibiting shear-induced coalescence. This excess is generally in the form of surfactant micelles in the continuous phase. These micelles dissociate into monomers that rapidly adsorb onto the surfaces of newly created droplets. The fourth requirement is that some form of extreme shear must be applied to rupture microscale droplets into nanodroplets. Typically, the stress level must reach the Laplace pressure of droplets having the desired size, usually in the range of 10–100 atm.

Extreme shear stresses in combination with the appropriate liquids and surfactant are rarely found in natural environments on the earth’s surface. In areas where oil seeps into the oceans, natural emulsions made by wave action are common, but droplet sizes rarely become submicron. It is possible that shear conditions appropriate for making nanoemulsions could exist below the earth’s surface, where liquids under high pressure could flow in porous rock; natural nanoemulsions of hydrocarbon oils and water might be found there. Neglecting this, nanoemulsions are a synthetic creation that would not likely exist otherwise except by human design and production.

Due to the large surface to volume ratio of droplet interfaces in nanoemulsions, the concentration of surfactant required to stabilize them is larger than for microscale emulsions, yet it is generally smaller than for lyotropic microemulsion phases. The concentration required for complete surface coverage can be crudely estimated by assuming an equilibrium surface density,  $\rho_s$ , for surfactant molecules on the droplet interfaces. In principle,  $\rho_s$  can depend on the bulk concentration of monomers in the continuous phase, but we assume that  $\rho_s$  is fixed and independent of  $C$ . As an example, we assume that the equilibrium surface concentration is roughly  $\rho_s \approx 1$  molecule/(20 Å<sup>2</sup>). If all droplets are spherical, the total number density of surfactant molecules per unit volume on the droplet interfaces is  $C_i = 3\phi\rho_s/a$ . For a dilute nanoemulsion of radius  $a = 50$  nm at  $\phi = 0.1$  stabilized by SDS, this corresponds to  $C_i \approx 10^{22}$  molecules cm<sup>-3</sup>  $\approx 20$  mM just to cover the surfaces. This concentration is well above the critical micelle concentration (CMC) of 8 mM for SDS. Given that surfactant must also be present in the bulk continuous phase as well as on the interfaces, the concentration of surfactant in solution required for fully populating the interfaces of nanoemulsion droplets range from tens to hundreds of millimolar. Since many surfactants form micelles at such high concentrations, it is usually the case that the continuous phase of nanoemulsions contains surfactant micelles as a reservoir of surfactant for coating the droplet interfaces. Although ensuring full surface coverage enhances the emulsion's stability, nevertheless, charge-stabilized droplets can remain stable at lower surface densities than those corresponding to equilibrium coverage.

Based on the Taylor estimate of the ruptured droplet radius, it is possible for us to predict the shear rates required to form nanoemulsions. First, we consider oil-in-water (i.e. water-based) emulsions, so  $\eta_c \approx 10^{-2}$  P, the viscosity of water. Assuming that the surface tension is  $\sigma = 10$  dyn cm<sup>-1</sup> and that we would like to produce droplets at the upper limit of the nanoscale regime with  $a = 100$  nm =  $10^{-5}$  cm, we predict that a shear rate of  $\dot{\gamma} \approx 10^8$  s<sup>-1</sup> is required. To obtain smaller droplets having  $a = 10$  nm, a larger shear rate of  $\dot{\gamma} \approx 10^9$  s<sup>-1</sup> would be needed. These shear rates are generally out of the range of most common mixing devices including high-speed blenders. Although some blenders may attain very high shear rates near the blade edges, the efficiency of bringing all droplets into this region is very low, and, therefore, this method is generally impractical. Given the inherent difficulties, only two methods for rupturing and dispersing droplets appear to be feasible for high-throughput production of water-based nanoemulsions: high-frequency ultrasonic devices and microfluidic devices. We cover the advantages and disadvantages of these approaches in the following paragraphs.

To finish our general discussion of the implications of Taylor's prediction for producing nanoemulsions, we now consider oil-based emulsions. Depending upon the molecular weight of the oil molecules and their interactions, the viscosity  $\eta_c$  can range from roughly that of water to many thousands of times that of water. Indeed, the oil molecules can even be made large enough that they entangle and the oil exhibits a shear-rate-dependent (i.e. non-Newtonian) viscosity [74, 75]. For simplicity, we only consider Newtonian liquids here. If, for instance, the oil's viscosity,  $\eta_c \approx 1$  P, is one hundred times that of water, then it would be possible to rupture droplets down to about 100 nm with a much lower shear rate of  $10^6$  s<sup>-1</sup>, attainable using a common blender. Figure 3 summarizes the scaling estimate for the droplet size as a function of shear rate for different  $\eta_c$ . Thus, water-in-oil nanoemulsions are typically easier to create than oil-in-water emulsions. Obviously, in common applications, the oil viscosity cannot be made arbitrarily large, otherwise the viscous torque on the motor of the blender will become too great for the motor to maintain its normal speed. However, if one wishes to make inverse nanoemulsions using oil that has a viscosity close to that of water, the following high-shear approaches for producing direct nanoemulsions could also be used for producing inverse nanoemulsions.

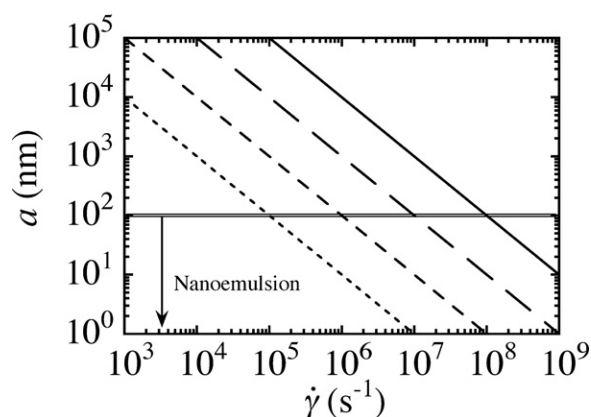


**Figure 3.** Estimate of the ruptured droplet radius,  $a$ , as a function of applied shear rate,  $\dot{\gamma}$ , based on Taylor's formula for emulsions having continuous phase viscosity  $\eta_c = 1$  cP (i.e. water) (solid line),  $\eta_c = 10$  cP (large-dashed line),  $\eta_c = 1$  P (medium-dashed line), and  $\eta_c = 10$  P (small-dashed line). Nanoemulsions having  $a \leq 100$  nm (i.e. below the horizontal double line) can typically be made only using extreme shear rates.

One method for producing nanoemulsions is through ultrasonic agitation of a premixed emulsion of microscale droplets [2]. The premixed emulsion has been made in advance using unsophisticated mixing methods to fix the composition of the emulsion (i.e.  $C$  and  $\phi$ ). In the ultrasonic method, a vibrating solid surface agitates the premixed emulsion at ultrasonic frequencies, typically 20 kHz or larger, and high power, causing extreme shear and cavitation that breaks up droplets. High-power ultrasonic devices include focusing horns and pointed tips. Since the emitted sound field is typically inhomogeneous, in most ultrasonic schemes, it is necessary to recirculate the emulsion through the region of high power so that all droplets experience the highest shear rate. Reasonably uniform droplet size distributions at dilute concentrations can be obtained if the emulsion is re-circulated many times through the region of high shear.

A second high-throughput method for producing uniform nanoemulsions involves using high-pressure microfluidic devices to rupture droplets in concentrated emulsions [1]. Rapidly flowing streams of a premixed emulsion are forced through rigid stainless steel microchannels, which have been fabricated using lithography and micromachining, to create an extremely strong extensional flow. The droplet sizes in the premixed emulsion are typically less than  $10 \mu\text{m}$ , and the channel dimensions are typically closer to  $100 \mu\text{m}$ . High-pressure air (typically around 100 psi) is mechanically amplified by a piston, which operates in a pulsed mode, to produce liquid pressures that can reach as high as about 30 000 psi (i.e. about 2000 atm). A premixed emulsion of microscale droplets is drawn at a volume rate of about  $Q \approx 3 \text{ ml s}^{-1}$  into a microfluidic channel and routed into an interaction area where an extreme extensional shear flow is created. Assuming that the channels have a width  $w \approx 75 \mu\text{m}$ , this corresponds to time-averaged shear rates of the order of  $\dot{\gamma} \approx Q/w^3 \approx 10^7$  to  $10^8 \text{ s}^{-1}$  and to peak shear rates around  $\dot{\gamma}_p \approx 10^8$  to  $10^9 \text{ s}^{-1}$ . These peak rates are large enough to create water-based nanoemulsions. Due to the spatial and temporal inhomogeneities of the pulsed microfluidic flow, it is generally necessary to recirculate the emulsion through the region of high shear or to pass it through the device several times; the number of passes is defined to be  $N$ .

The advantage of this 'high-throughput microfluidic nanoemulsification' method is the combination of extremely high peak shear rates, high-volume throughput of nanoscale droplets

at relatively large  $\phi < 0.6$ , and reasonably uniform droplet size distributions having  $\delta a/\langle a \rangle < 0.2$ . This relatively low polydispersity is comparable to that which can be produced by ultrasonic methods that also include recirculation. Indeed, in the microfluidic method, the peak shear rates can be so large that it is possible to heat the emulsion significantly above room temperature through viscous dissipation alone. Heating water by dissipation of shear energy is not easy to achieve, especially given the high heat capacity of water, yet this heating provides a very tangible example of just how much shear is usually required to create water-based nanoemulsions. If such heating is not desired, the product nanoemulsion that leaves the region of extreme shear can be cooled using a heat exchanger without affecting the size distribution or stability. Moreover, the volume rate of production of the nanoemulsion can be quite high, reaching rates of many litres per hour. Depending upon the final nanodroplet radius after rupturing, this implies that the production rate ranges from about  $10^{14}$ – $10^{18}$  droplets per second.

Although hydrodynamic focusing of a liquid jet of the dispersed phase surrounded by the continuous phase in soft microchannels at low pressure can be used to produce very uniform submicron droplets [28], in comparison to the previous high-pressure microfluidic method, the rate of production of nanoscale droplets is quite low. This low-pressure focusing method appears to be most appropriate for low-throughput specialty applications requiring a very high degree of monodispersity, yet very small total droplet volume. Moreover, the shear rates required to produce 10 nm droplets using flow focusing would typically require high injection pressures that will most likely destroy microfluidic devices made using soft lithography (e.g. silicone-based microchannels). Consequently, hard lithographic microchannels would almost certainly be needed to approach the lower end of the nanoscale droplet regime [76]. Another potential source of nanoscale droplets is tiny satellite droplets that can form during the capillary-driven breakup of larger microscale droplets in the production of conventional emulsions [20]. Such secondary satellite droplets are technically nanoemulsions, yet their rate of production is generally miniscule when compared to either the high-throughput microfluidic or the ultrasonic methods.

As an example of the high-pressure microfluidic approach, we highlight some recently reported results that detail the creation of silicone oil-in-water nanoemulsions stabilized by SDS [1]. This systematic study clearly shows how varying the composition and shearing conditions can be used to control the droplet size distribution, measured using DLS. The silicone oil (polydimethylsiloxane or PDMS) we have used has a large enough molecular weight that its solubility in the water phase is very small and can be neglected. As an example of the evolution of the droplet size distribution as a function of the number of passes, in figure 4(a), we show the volume-weighted probability distribution for the radius,  $p(a)$ , as the emulsion has been passed through the region of high shear. The premixed emulsion, made using a simple blender, has  $C = 116$  mM,  $\phi = 0.2$ ,  $\eta_d = 10$  cP, and the input air pressure, which controls the peak shear rate, has been fixed at  $p = 130$  psi. As the number of passes increases, the mean and standard deviation of  $p(a)$  both decrease and then saturate (figure 4(b)). We define these quantities to be saturation radius,  $\langle a_s \rangle = \langle a(N \rightarrow \infty) \rangle$ , and the saturation standard deviation,  $\delta a_s = \delta a(N \rightarrow \infty)$ . Passing the nanoemulsion through the region of extreme shear multiple times increases the uniformity and decreases the mean size primarily because all droplets eventually experience the highest peak shear rate the pulsed flow can create.

In the extreme shearing conditions required to produce nanoemulsions, the droplet volume fraction can strongly affect the resulting droplet size distribution in a way that has not been previously seen with microscale emulsions. In figure 5, the saturation radius remains relatively constant at low  $\phi$ , yet it increases as  $\phi$  becomes larger. As  $\phi$  approaches  $\phi_{MRJ}$ , the droplet size begins to increase dramatically, and the emulsion inverts from a water-continuous to an

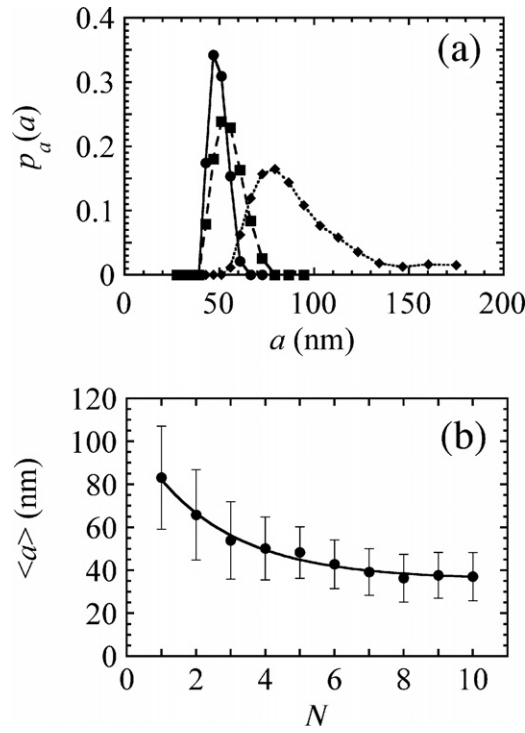


**Figure 4.** (a) Droplet size distribution of emulsions,  $p(a)$ , measured using dynamic light scattering after  $N = 1$  ( $\blacklozenge$ ), 3 ( $\blacksquare$ ), and 5 ( $\bullet$ ) passes through the high-pressure microfluidic device at a volume fraction  $\phi = 0.2$ , concentration of sodium dodecylsulfate  $C = 116$  mM, oil viscosity  $\eta_d = 10$  cP, and air pressure  $p = 130$  psi. (b) Average radius  $\langle a \rangle$  as a function of  $N$ . The solid line is a fit to a decaying exponential plus a constant, the saturation radius  $\langle a_s \rangle = \langle a(N \gg 1) \rangle$ . (From [1], © 2004 by Taylor and Francis, used with permission.)

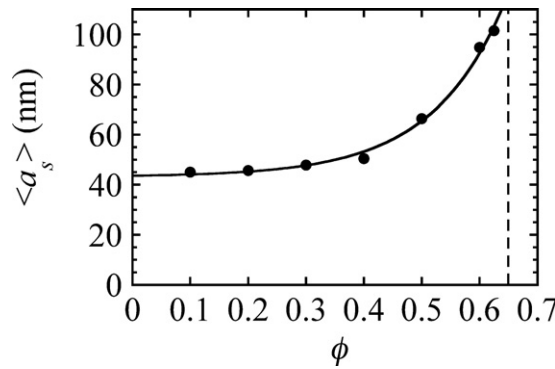


**Figure 5.** Average droplet radius for large number of passes,  $\langle a_s \rangle$ , as a function of  $\phi$ . Phase inversion of the emulsion occurs for  $\phi \geq 0.64$  (dashed line). (From [1], © 2004 by Taylor and Francis, used with permission.)

oil-continuous emulsion for  $\phi > \phi_{MRJ}$ . This trend is contrary to what the following simple argument, based on rheological properties of the emulsion alone, would predict. Naively, one might argue that the presence of droplets at larger  $\phi$  should raise the effective viscosity

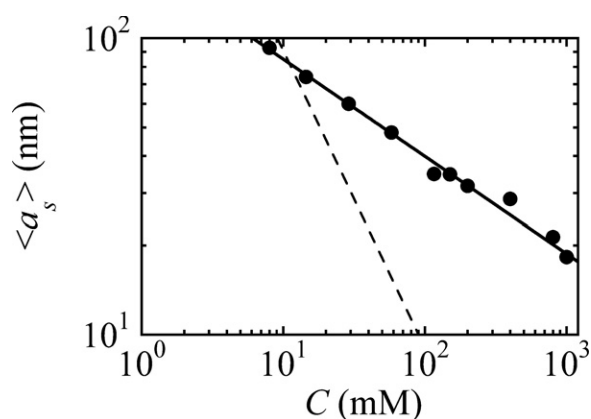


**Figure 6.** Average droplet radius,  $\langle a_s \rangle$ , as a function of SDS concentration,  $C$ , at fixed volume fraction  $\phi = 0.2$ , air pressure  $p = 130$  psi, and oil viscosity  $\eta_d = 10$  cP. The solid line is an empirical fit to  $\langle a_s(C) \rangle \sim C^{-1/3}$ . The dashed line shows the predicted radius of droplets that are fully covered with surfactant at a fixed surface density of  $20 \text{ \AA}^2$  per head group:  $\langle a \rangle \sim 3\phi\rho_s/C$ . (From [1], © 2004 by Taylor and Francis, used with permission.)

of the emulsion. Therefore, at the same shear rate, the viscous stress available to rupture droplets would be larger. Since Taylor's estimate is inversely proportional to the viscous stress, this would suggest that the average ruptured droplet size should decrease as  $\phi$  increases. Overall, this argument is reasonable, yet it makes a primary assumption that may not hold for droplets in a high-shear environment. This assumption is that the repulsive stabilization between droplet interfaces provided by the surfactant is strong enough to inhibit coalescence when droplets are strongly forced into neighbouring droplets by the extreme shear. One can imagine a situation in which the droplets become concentrated enough that the strong shear which drives them into nearby neighbouring droplets actually overcomes the disjoining pressure and causes the droplets to merge; this phenomenon is known as 'shear-induced coalescence' [77]. The experimental evidence in figure 5 clearly shows that understanding and controlling shear-induced coalescence is of primary importance in nanoemulsification. Clearly, more investigation is needed to determine how shear-induced coalescence alters the size distribution of droplets ruptured at high volume fractions in extreme shear both quantitatively and theoretically.

The concentration of surfactant in the solution can also play an important role in determining the saturation radius of the droplets resulting from emulsification when all other parameters are fixed. In figure 6,  $\langle a_s(C) \rangle$  decreases as  $C^{-1/3}$  (solid line) over two decades in  $C$ , from the CMC of SDS to the maximum saturation concentration at room temperature. It is not clear whether the observed scaling has a fundamental, but as yet undiscovered, mechanism that gives rise to a power law exponent of  $-1/3$ , or whether the trend is merely fortuitous. At such large concentrations of surfactant, the micellar phases that form increase the effective viscosity of the continuous phase and, according to the Taylor estimate, would therefore lead to a reduction in  $\langle a \rangle$ ; likewise, higher  $C$  is also known to cause a reduction in  $\sigma$ . The combination of these two effects could lead to the observed reduction without appealing to other mechanisms, but this hypothesis remains to be tested. For reference, we show the predicted surfactant concentration  $C_i \approx 3\phi\rho_s/\langle a_s \rangle$  required to coat the surfaces of the droplets, assuming  $\rho_s$  is fixed (see dashed line in figure 6). Since this line falls below the measured trend, there is a possibility that the equilibrium surface density of the SDS on highly curved nanodroplet interfaces may deviate from the surface density on flat interfaces. Another possibility is that

the rate of adsorption of the surfactant from the bulk onto droplets after they are ruptured may play an important role; if the droplet interfaces are not coated quickly enough, shear-induced coalescence could be limiting the ultimate attainable size. Clearly, more systematic investigations with other surfactant types, including rheological characterization, as well as measurements of interfacial tension and surface density on curved interfaces, are needed to resolve these interesting issues. What is clear from these experiments, however, is that it is possible to produce bulk quantities of oil nanodroplets in water that have relatively uniform size distributions with average radii down to about 15 nm.

The influence of the dispersed phase viscosity on the high-pressure microfluidic emulsification process has also been explored. It is possible to make nanoemulsions out of silicone oils having higher viscosities, up to 1000 cP, although the droplet sizes are several times larger for the more viscous oils [1]. This variation is likely due to the higher viscous stresses resisting the rupturing of stretched droplets as the capillary instability unfolds. This observation confirms that direct nanoemulsions can be made using a broad range of molecular weight oils. It also confirms that the dominant force resisting droplet deformation is due to the interfacial tension, not viscous dissipation inside the droplets, at least for low molecular weight oils.

Measurements of the shear-induced coalescence of macroscopic droplets [77] are likely to improve the relatively limited theoretical understanding of this important phenomenon. Shear-induced coalescence can have a large impact on the size distributions of nanoemulsions [1]. Although it would be nice to directly image the stretching, rupturing, and coalescing processes of nanoscale droplets using high-speed cameras, the timescales are so short that even the best technology cannot capture the very fast processes that would occur. One can estimate the rupturing time for a 100 nm droplet to be of the order  $\eta_d/\Pi_L \approx 10^{-8}$  s, assuming  $\eta_d > \eta_c$ . Thus, learning about shear-induced coalescence from real-space visualization of larger microscale or macroscale droplets and then examining how the rules would impact the size distributions of nanoscale droplets appears to be the most reasonable approach.

In summary, extreme shear can be used to transform microscale emulsions into nanoemulsions through microfluidic and ultrasonic processes. White premixed emulsions comprised of microscale droplets can be turned into translucent nanoemulsions that can remain stable against coarsening almost indefinitely. Whereas it is possible to emulsify microscale and larger droplets at volume fractions well above  $\phi_{MRJ}$ , shear-induced coalescence can make the creation of nanoemulsions at such large  $\phi$  problematic. More research is clearly needed to understand the origin of the changes in the saturation droplet radius as a function of composition and shearing conditions.

### 3. Manipulating nanoemulsions

Once nanoemulsions have been formed, it is possible to manipulate them in a variety of useful ways. In this section, we describe methods for improving the uniformity of the size distribution through ultracentrifugal fractionation, for altering the volume fraction, surfactant concentration, and composition of the continuous phase, and for preparing controlled nanoemulsions suitable for scattering studies of structure.

Polydisperse nanoemulsions can be separated by size into several more monodisperse nanoemulsions in a process known as fractionation [78]. One useful method for fractionating microscale droplets is through depletion attractions induced by surfactant micelles [79, 6, 17]. Large droplets aggregate and cream whereas small droplets remain unaggregated and thermally dispersed. By repeatedly separating the cream, diluting the droplets, and raising the surfactant concentration to a different value, it is possible to obtain highly monodisperse emulsions [80].

Although this depletion attraction approach can be used to fractionate droplets that are in the upper limits of the nanoscale regime, it is generally ineffective for most nanoemulsions due to the extremely small droplet sizes, which can become comparable to the micellar size. Despite adding very large quantities of surfactant to raise the osmotic pressure exerted by the micelles on the droplets, the depletion attraction between nearby nanodroplets remains less than thermal energy, so the aggregation of nanodroplets does not occur. Empirically, for SDS-stabilized oil-in-water emulsions, depletion fractionation works down to about  $a \approx 100$  nm. As a result, a different method of fractionation is required for nanoemulsions.

Centrifugal size separations of particulate dispersions and cell contents have been performed for many decades [81]. To fractionate the size distribution of nanoemulsions, we simply use ultracentrifugation at very high rotation rates. If the droplets in the nanoemulsion are spherical, they experience a buoyant force,  $F_b = (4\pi a^3/3)\Delta\rho g$ , where  $\Delta\rho = \rho_d - \rho_c$  is the difference in mass density between the dispersed and continuous phase liquids and  $g$  is the effective acceleration (i.e. 'gravity') generated by the ultracentrifuge. For many oil-in-water emulsions  $\Delta\rho$  is negative, so the droplets cream rather than settle. After initial transients have died away, the viscous drag force on the droplet is  $F_d = 6\pi\eta_c a v$ , where  $v$  is the steady state velocity of a droplet. At steady state, if we neglect thermal forces, the buoyant force is opposed by the viscous drag force, and the velocity is [4]  $v = 2a^2\Delta\rho g/(9\eta_c)$ . Thus, since the velocity is proportional to  $a^2$ , larger droplets will cream (or settle) much more rapidly than smaller droplets.

The large difference in the creaming velocities provides an efficient means of separating large nanodroplets from smaller ones. Assuming  $\Delta\rho = -0.05$  g cm<sup>-3</sup> and the effective acceleration generated by the centrifuge is  $g = 10^7$  cm s<sup>-2</sup>, nanodroplets having  $a = 100$  nm in water will attain a steady velocity of roughly  $|v| \approx 10$   $\mu$ m s<sup>-1</sup>. Such droplets will cream over distances of about 10 cm in about  $10^4$  s  $\approx 3$  h. Thus, for a tube several centimetres long, running the ultracentrifuge for several hours at 20 000 RPM is typically sufficient to cause the 100 nm droplets to cream. For the same conditions, smaller nanodroplets having  $a = 10$  nm will reach a velocity of only  $v = 10^{-1}$   $\mu$ m s<sup>-1</sup>. This velocity is so small that it would require  $10^5$  s  $\approx 1$  day to cause them to cream 1 cm. Since thermal forces also act to keep the droplets dispersed, several days of ultracentrifuging can be required to cream the very smallest nanodroplets. After ultracentrifugation, the droplets are recovered as a solid plug at the top of the centrifuge tube. The lower part of this plug contains smaller droplets and the top part of the plug contains the larger droplets (figure 7). The volume fraction in the plug is also non-uniform; for creaming,  $\phi$  is typically smaller toward the bottom of the plug, since the applied osmotic pressure is weaker there. By cutting the plug into sections, re-dispersing, and re-centrifuging, highly uniform nanoemulsions at the large end of the lengthscale range can be obtained. Thus, successive ultracentrifugation steps can be used to fractionate the size distribution by taking advantage of size-dependent creaming rates.

Often, it is desirable to alter the composition of the uniform nanoemulsion after fractionation. This includes adjusting  $\phi$  and  $C$ , substituting surfactants that have not been used during emulsification, and performing solvent exchange of the continuous phase. The procedures outlined below are common to many types of colloidal dispersions once they have been formed, and nanoemulsions are no exception.

The droplet volume fraction can be lowered simply by dilution. Diluting with the pure continuous-phase liquid reduces both  $\phi$  and  $C$  simultaneously. With certain surfactants, it is conceivable that the reduction in  $C$  could cause the surfactant to desorb from the interfaces, leading to destabilization of the nanoemulsion. If ionic surfactants are used, the charge repulsion of the interfaces is usually strong enough that destabilization will not occur upon dilution with the pure continuous phase. Regardless of the type of surfactant, it is usually

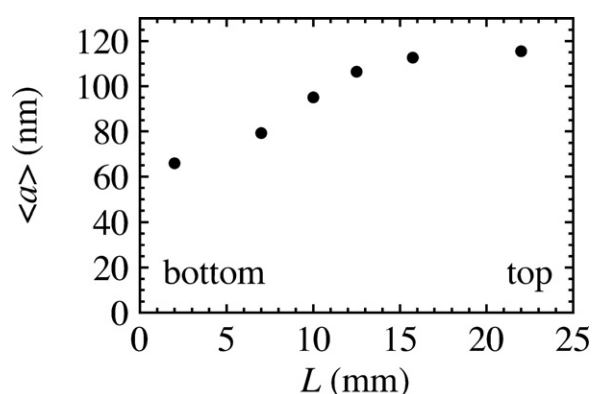


**Figure 7.** Average droplet radius,  $\langle a \rangle$ , as a function of length,  $L$ , along the solid plug of concentrated emulsion after ultracentrifuging a silicone oil-in-water nanoemulsion at 20 000 RPM for 3 h. Small and large  $L$  correspond to the bottom and top of the plug, respectively. (From [78], © 2006 Mason, used with permission.)

prudent to dilute with a surfactant solution to maintain  $C$  while lowering  $\phi$ . After diluting a nanoemulsion comprised of repulsively interacting droplets, thermal energy will ultimately cause the volume fraction to equilibrate and become homogeneous everywhere. However, since diffusion is a slow process, in most practical situations and especially for concentrated elastic nanoemulsions, it is advisable to stir after diluting in order to facilitate the complete dispersal of droplets.

Ultracentrifugation and dialysis are common methods for applying osmotic pressures to raise  $\phi$ . The recovered plug of nanoemulsion from a centrifuge tube generally contains a gradient in volume fraction: higher  $\phi$  at the top of the plug because of the pressure due to all the droplets underneath and lower  $\phi$  at the bottom of the plug since relatively few droplets are below to press on the layers of droplets above. Eventually, the volume fraction and osmotic pressure in the plug will equilibrate, but this can be a slow process. Therefore, it is usually necessary to stir the contents of the plug in order to speed up the equilibration by bringing regions having different  $\phi$  into close proximity. In dialysis, the dilute nanoemulsion is placed in a semi-permeable bag, and this bag is clipped, sealed, and immersed in a polymer–surfactant solution which has a strong affinity for molecules of the continuous phase. Thus, molecules of the continuous phase leave the emulsion to further dilute the polymer on the other side of the membrane. Care in selecting the molecular weight cutoff of the bag is necessary to avoid a situation in which nanodroplets can escape. Likewise, if the dialysis liquid is devoid of surfactant, and if the surfactant can traverse the dialysis membrane, then destabilization of the nanoemulsion could occur through an unintended reduction in  $C$ . By contrast to ultracentrifugation, dialysis is usually a slow process and large gradients in  $\phi$  do not develop in the nanoemulsion while it is being compressed in the dialysis bag.

Sometimes it is desirable to change the concentration or even the type of surfactant used to stabilize the nanoemulsion. The following procedure can be used to control  $C$  and  $\phi$  independently. A stock solution at the desired bulk surfactant concentration is made. The nanoemulsion droplets are concentrated by osmotic pressure and then diluted using this stock solution. After repeating the process of concentration and dilution with the stock solution, one can fix  $C$  to the desired value. It is then necessary to measure  $\phi$  after a final concentration step. This measurement can be achieved by simply evaporating a small portion of the sample. Non-destructive measurement of  $\phi$  is generally more difficult, but  $\phi$  can be inferred through

pycnometry, light scattering, or neutron scattering methods. Once  $\phi$  of the concentrated emulsion has been determined, it is then simple to dilute to the desired  $\phi$  using a stock solution. Obviously, this procedure can be used to alter the type of the surfactant as well, provided that the pre-existing surfactant can readily desorb from the droplet interfaces. The continuous phase liquid can also be exchanged out, provided the desired continuous phase is readily miscible with the pre-existing continuous phase. This method has been used to prepare silicone oil-in-D<sub>2</sub>O nanoemulsions suitable for neutron scattering from an original silicone oil-in-H<sub>2</sub>O nanoemulsion [82–84].

In summary, the droplet size distribution and composition of nanoemulsions can be controlled to a high degree once the extreme emulsification process has been completed. Thus, nanoemulsions are a very flexible physical system, and many possibilities exist for interesting chemical substitutions.

#### 4. Structure of nanoemulsions

Understanding the physical properties of nanoemulsions can be difficult unless one develops a clear picture of droplet structure, so we establish basic concepts of the positional and interfacial structures of repulsive and attractive nanoemulsions in this section. We introduce the concept of a ‘nanoemulsion glass’, a frustrated and disordered arrangement of concentrated nanodroplets that never reach an equilibrium structure, and we review recent experiments that reveal the bulk structure of nanoemulsion glasses over a wide range of  $\phi$  [82, 83]. At the very highest  $\phi$ , the droplets can deform significantly into structures that resemble random monodisperse foams. This is a very interesting area, since experimental determination of the bulk structure of random foam has not been adequately measured. We also describe the recently reported phenomenon of dense cluster formation in slippery diffusion-limited cluster aggregation, or ‘slippery DLCA’, that occurs when nanoemulsion droplets become strongly attracted to each other [84].

A complete structural description of a nanoemulsion would involve specifying the surfaces defined by the droplet interfaces everywhere in the sample. This is a tremendous amount of information, and some simplification is necessary in order to more conveniently discuss the structure. In treating nanoemulsions as dispersions of deformable droplets, it is convenient and appropriate at low  $\phi$  to assume that the interfacial structures of the droplets are spherical. This is typical when the nanoemulsion experiences a moderate shear such that  $\Pi_L$  remains much greater than  $\tau$ . For a monodisperse system of droplets, the entire interfacial structure can then be completely specified by the positions of the centres of all of the droplets and the unique droplet radius. This set of positions can be referred to as the ‘droplet positional structure’. In many cases, it is possible to further reduce the required information by specifying the pair correlation function,  $g(r)$ , a statistical quantity that can be computed by considering the relative positions of pairs of droplets in the nanoemulsion separated by a centre-to-centre distance  $r$  [85]. Although the pair distribution function is convenient to compute from real-space observations, it can be Fourier transformed to provide the structure factor,  $S(q)$ , where  $q$  is the wavenumber associated with a neutron or x-ray scattering experiment. In many cases, it is far more convenient to measure the structure factor than to perform cryo-EM on a vitrified sample to examine the interfacial structure in a thin layer (e.g. in TEM) or at a fracture plane (e.g. in cryo-fracture SEM). By contrast, at high  $\phi$  above  $\phi_{MRJ}$ , the simplifying assumption that the droplets are spherical cannot be made, and describing the interfacial structure of the nanoemulsion only by centre positions of the droplets becomes inadequate. In this case, when droplets become deformed, it is necessary to describe all of the details about the interfacial surfaces in the emulsion, and any measurement of a structure factor by scattering is not strictly valid.

Coherent neutron and x-ray scattering are excellent methods for probing the bulk structure of nanoemulsions. Using short wavelengths,  $\lambda < 10 \text{ \AA}$ , compared to the droplet size, it is possible to obtain accurate measurements of the structure factor. Neutron scattering offers the additional advantages that the intensity is reported in absolute calibrated units (typically  $\text{cm}^{-1}$ ), there is a relatively flat background scattering known as incoherent scattering, and the neutron scattering contrast between the droplets and the continuous phase can be altered significantly by simple solvent exchange. As an example, we consider a repulsive silicone oil-in- $\text{D}_2\text{O}$  nanoemulsion that has been fractionated and subsequently solvent-exchanged [82, 83]. Concentration of the nanoemulsion by centrifugation leaves the droplets in a disordered glassy configuration, so all scattering patterns are uniform about the beam stop, and azimuthal averages of intensity counts on a two-dimensional detector are appropriate. A measurement of the intensity,  $I$ , as a function of scattering wavenumber,  $q$ , at very dilute  $\phi$  to obtain the form factor,  $F(q)$ , is followed by a measurement of  $I(q)$  at the volume fraction of interest. In the case where  $\phi$  is low enough that droplet deformation does not occur, the structure factor can be obtained simply:  $S(q) = I(q)/F(q)$  [71]. However, when  $\phi$  is large enough that the droplets begin to deform, this simple quotient for determining  $S$  is not strictly valid because the form factor of a deformed droplet is different than the form factor of an undeformed spherical droplet. Therefore, the structure factor calculated through naive division is only effective when droplets are deformed [83].

An example of the form factor for a fractionated nanoemulsion of repulsive droplets at  $\phi = 0.005$  measured using small angle neutron scattering (SANS) is shown in figure 8(a) (small circles and solid line). A plateau at low  $q$  decreases rapidly at a value roughly corresponding to the inverse droplet radius, and a subsequent smaller shoulder at higher  $q$  also decays. Perfectly monodisperse spheres show very dramatic minima and maxima that modulate the decay of the form factor towards higher  $q$ . Since the form factor is essentially a Fourier transform of a sphere, these interference oscillations are expected. If the nanoemulsion has a significant size polydispersity and if the source of neutrons has a significant spread of wavelengths, then these abrupt oscillations can be smeared out, yielding smoother bumps and shoulders. Neglecting the wavelength spread, the measured form factor can be fitted to a superposition of predicted form factors for spheres having different sizes to determine the radial size distribution. A line showing the fit provides a mean radius of  $\langle a \rangle = 77 \text{ nm}$ , consistent with dynamic light scattering, and a standard deviation  $\delta a = 10 \text{ nm}$ , yielding a polydispersity of  $\delta a / \langle a \rangle = 0.13$ .

As an example of determining the structure factor at higher  $\phi = 0.67$ , we show the measured intensity,  $I(q)$ , as a function of  $q$  (figure 8(a)—solid squares). The form factor is then matched to the coherent scattering at high  $q$ , and the two functions are divided to give  $S(q)$ , shown in figure 8(b). At very low  $q$ , the value of  $S(q)$  is significantly below unity due to the impenetrability of the droplets, and this matches predictions for Percus–Yevick hard spheres [86, 87]. This is not so surprising, since the Debye screening length,  $\lambda_D$  [88], for this nanoemulsion is only about  $\lambda_D \approx 3 \text{ nm}$ ; therefore, undeformed droplets resemble hard spheres to a reasonable degree. However, at larger  $q$ , the peak indicates spatial correlations in the positional structure of the droplets.

Detailed measurements of the effective structure factor of osmotically compressed monodisperse nanoemulsions [83] show that hard sphere theory properly describes the low  $q$  limit of  $S$ , at least up to  $\phi$  associated with the glass transition. The behaviour of the peak in the effective  $S(q)$  as a function of  $\phi$  has been measured, and the peak value goes through a maximum as  $\phi$  is increased and can even lead to sub-unity peaks at  $\phi$  beyond the glass transition. It is possible that interference effects associated with the thin films of liquids can lead to slight alterations of the tail of  $I(q)$  at large  $q$ , thereby leading to the sub-unity peaks in the effective  $S(q)$  when  $F(q)$  and  $I(q)$  at high  $q$  are empirically matched and divided.

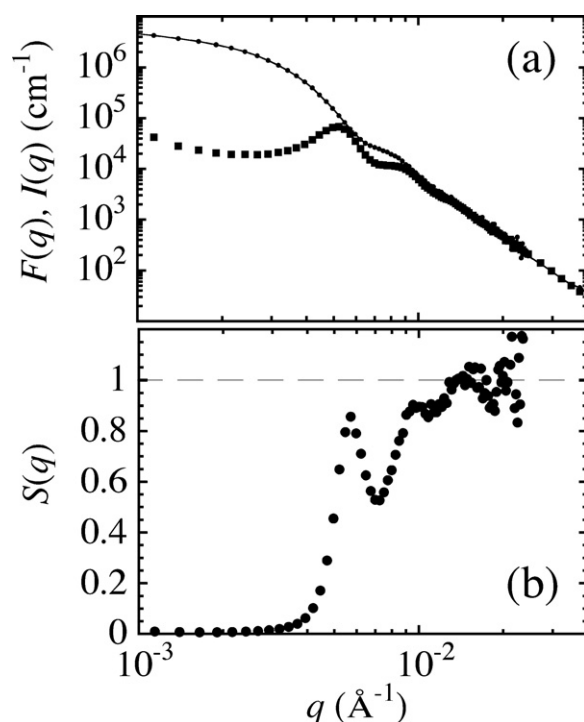


**Figure 8.** (a) Measured small angle neutron scattering (SANS) intensity as a function of wavenumber,  $I(q)$ , of a concentrated silicone oil-in-water nanoemulsion at  $\phi = 0.67$  (squares). The neutron wavelength is  $\lambda = 8 \text{\AA}$ . The form factor,  $F(q)$ , measured at a dilute concentration of  $\phi = 0.005$  (small circles and solid line) has been scaled by a constant factor so that  $I(q) = F(q)$  for large  $q$ . A fit to the form factor yields  $a = 77 \pm 10 \text{ nm}$ . (b) The effective structure factor,  $S(q)$ , obtained from the ratio  $I(q)/F(q)$  shown in part (a). (From [83], © 2006 by American Chemical Society, used with permission.)

Although several hypotheses exist, these interesting trends in the structure of nanoemulsion glasses at large  $\phi$  remain largely unexplained, and theoretical interpretations that include droplet deformability are being examined to determine their origin.

Inducing attractive interfacial interactions that do not cause droplet coalescence can cause dramatic changes in the structure of nanoemulsions. In the absence of attractive interactions, nanoemulsions are homogeneous dispersions. By contrast, when strong attractive interactions relative to thermal energy are present, the droplets aggregate and large-scale spatial inhomogeneities form in the emulsion. Detailed studies of this aggregation process for an attractive nanoemulsion system have been reported [84]. The attraction is introduced by adding salt (NaCl) to an SDS-stabilized silicone oil-in- $\text{D}_2\text{O}$  nanoemulsion and quenching the temperature over a small range. At high temperatures, the droplets remain dispersed and the attraction is very weak, yet, below a critical temperature  $T^*$ , the short-range interfacial attraction between the droplets becomes much stronger than the thermal energy. Thus, by quenching the temperature  $T$  below  $T^*$  and measuring  $I(q)$  over time,  $t$ , using time-resolved SANS, the evolution of the structure of the nanoemulsion has been recorded during the aggregation and gelation process. For  $0.05 < \phi < 0.25$ , the authors have shown that the aggregation leads to the formation of peaks at high  $q$  associated with attractive jamming of droplets and a well-defined separation between droplets in jammed clusters (figure 9—arrows).

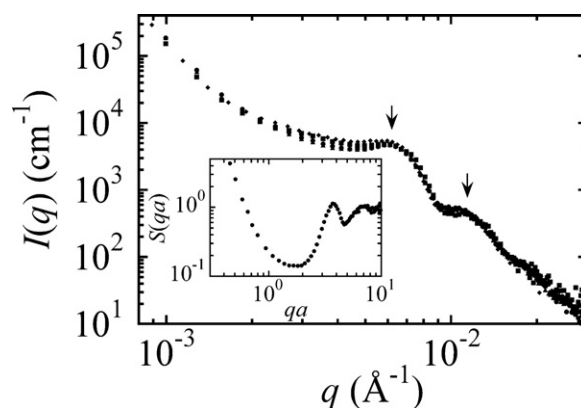


**Figure 9.** Long-time SANS intensity,  $I(q, t \rightarrow \infty)$ , characteristic of slippery diffusion-limited cluster aggregation for droplet volume fractions,  $\phi = 0.05$  (●),  $0.12$  (■),  $0.20$  (◆),  $0.27$  (▲). The data at lower  $\phi$  have been rescaled onto a master curve with absolute intensity corresponding to  $\phi = 0.27$ . The droplet radius is fixed:  $\langle a \rangle = 51 \pm 8$  nm. Cluster peaks are evident at high  $q$  over a wide range of  $\phi$  (arrows). Inset: the universal structure factor as a function of dimensionless wavenumber,  $S(qa)$ . (From [84], © 2006 by American Physical Society, used with permission.)

After the dense clusters have formed,  $S(q)$  at low  $q$  grows more slowly as the larger-scale fractals comprised of dense clusters eventually form a gel. Moreover, the structure factor over this range of  $\phi$  appears to be universal (figure 9—inset).

From these experiments on attractively quenched nanoemulsions, the very general and important concept of slippery DLCA has been clearly revealed [84]. In this process, droplets aggregate into dense clusters because the attractive bonds they form with other droplets are not shear rigid. As a result, droplets must first form small rigid building blocks, such as tetrahedra, before these rigid building blocks of dense clusters can aggregate in a traditional diffusion-limited manner to form fractal clusters and gels. Although the fractal dimension of slippery DLCA clusters is not very different from that of traditional DLCA of solid particulates that form shear-rigid bonds [89, 8], the average coordination number (i.e. number of nearest neighbours per droplet) of slippery DLCA is much higher, leading to more pronounced peaks in the structure factor at high  $q$ . This example highlights how nanoemulsion science is advancing the frontiers of our general understanding of the structure of soft matter.

Small-angle x-ray scattering (SAXS) can also be used to probe nanoemulsion structure. An example of  $I(q)$  for a fractionated silicone oil-in-water nanoemulsion at  $\phi = 0.055$  is shown in figure 10. Here, the large number of oscillations is indicative of a high degree of uniformity of the droplet size distribution. Although the peaks clearly indicate strong positional correlations of the disordered droplets, the absolute intensity is not directly comparable to theoretical models, since it must first be corrected for a  $q$ -dependent background known as ‘parasitic scattering’ [71]. The relatively high scattering intensities should also make dynamic x-ray scattering experiments, known as x-ray photon correlation spectroscopy (XPCS), possible.

One interesting and exciting advance in the area of real-space determination of the structure of nanoemulsions is through continuous phase evaporation-TEM. In this simple method, a silicone oil-in-water nanoemulsion is stained with depleted uranyl acetate, placed on a TEM grid coated with a monolayer polymer film, the water is evaporated, and the sample is observed at room temperature using TEM. If the droplets are at dilute  $\phi$ , they do not completely cover the grid, and they do not coalesce during the evaporation (most likely due to the stain). It is even possible to observe nanoemulsion droplets that have been concentrated and deformed during

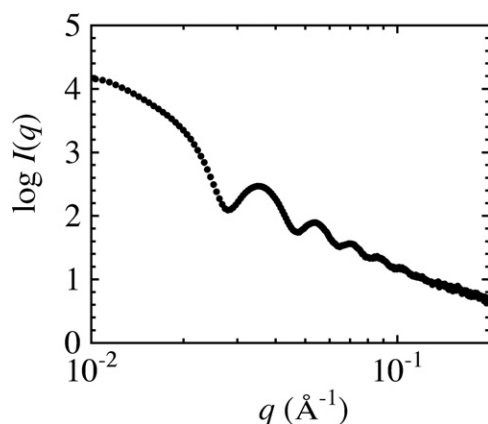


**Figure 10.** Small-angle x-ray scattering (SAXS) intensity,  $I(q)$ , of highly fractionated nanoemulsions having  $\langle a \rangle = 16 \pm 4$  nm at a concentration of  $\phi = 0.055$  exhibits multiple peaks characteristic of diffraction from uniform spheres. The x-ray wavelength is  $\lambda = 1.4$  Å.

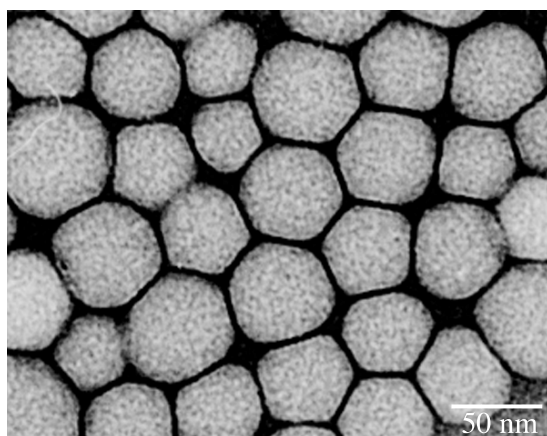


**Figure 11.** Transmission electron micrograph of concentrated silicone oil nanodroplets after staining with uranyl acetate and evaporating the aqueous phase. The foam-like structure of the concentrated droplets is evident.

the evaporation process (figure 11). The silicone oil has a large enough molecular weight that it is not expected to significantly evaporate under the conditions used. Although the reason why this simple method provides such nice results is still being evaluated, we believe that this is the first clear real space evidence for a foam-like structure of nanoscale droplets that have been concentrated to high  $\phi$ . Moreover, image analysis of scanned TEM films can provide accurate number-weighted size distributions.

Scattering and real-space studies of fractionated nanoemulsions are beginning to provide the essential understanding of the positional structure and deformation of droplets in these important systems. Droplet size distributions and positional structures can be measured using SANS or SAXS. Traditional cryo-EM and non-traditional evaporation-TEM can provide real space nanodroplet structures. These structures are related to the droplet volume fraction, droplet size distribution, and the interaction between the droplets. A basic understanding of the

structures of attractive and repulsive nanoemulsions have given rise to the concepts of slippery DLCA and disordered nanoemulsion glasses.

## 5. Physical properties of nanoemulsions

Nanoemulsions have many interesting physical properties that are different from or are more extreme than those of larger microscale emulsions. In this section, we focus on a few of the physical properties that distinguish nanoemulsions from microscale emulsions as an important new class of soft materials. We examine the relative transparency of nanoemulsions, their response to mechanical shear or ‘rheology’ [74, 75], and the enhanced shelf stability of nanoemulsions against gravitationally driven creaming. We do not intend to provide a comprehensive review of all of the possible properties, but these particular properties serve as a few primary examples.

Nanoemulsions appear visibly different from microscale emulsions since the droplets can be much smaller than optical wavelengths of the visible spectrum (figure 12—inset). Microscale emulsions multiply scatter visible light [90], and unless the refractive index of the continuous and dispersed phases are matched by specifically altering the composition to achieve this, they appear white. By contrast, nanoemulsions can appear nearly transparent in the visible spectrum and exhibit very little scattering despite significant refractive index contrast. Quantitative measurements of the optical transparency of nanoemulsions in the visible and ultraviolet wavelengths are shown through transmission measurements in figure 12. Nanoemulsions having  $a = 40$  nm at several different  $\phi$  have been loaded into 0.2 mm pathlength quartz cells, and the per cent transmission intensity has been measured as a function of light wavelength. For all  $\phi$ , the transmission in the visible spectrum is near 100%, especially toward red wavelengths, indicating a high degree of transparency. By contrast, in the ultraviolet (UV) part of the spectrum, as the wavelength of light begins to approach the droplet radius, the nanoemulsions scatter light significantly. As  $\phi$  increases from the dilute regime up to about  $\phi \approx 0.13$ , the transmission in the ultraviolet drops as the number of scatterers increases, yet at higher  $\phi > 0.13$ , the UV transmission increases again, indicating that more concentrated emulsions scatter less light. This increase and subsequent decrease in the scattering of light by the droplets as  $\phi$  is increased arises from the behaviour of the nanoemulsion’s structure factor in the low  $q$  (transmission) limit. In effect, correlations in the droplet positional structure cause the increased transparency at higher  $\phi$ . The smaller the droplet radius, the broader the range of visible wavelengths over which the transparency is found, especially toward the blue and the ultraviolet wavelengths.

In the limit when the nanodroplets are much smaller than the wavelength of the incident light, one encounters the regime of ‘Rayleigh scattering’ [90]. Rayleigh scattering gives rise to the blue sky when looking away from the sun during the day and the red sky when looking toward the sun as rays pass through very large distances of the atmosphere during sunset. In this form of scattering, polarizable matter much smaller than the wavelength of light has a scattering cross section that is inversely proportional to the fourth power of the wavelength. Nanoemulsions comprised of droplets with  $a \ll 400$  nm exhibit scattering similar that arising from polarizable molecules in the atmosphere. Nanoemulsions appear transparent, yet a bit bluish due to the dominance of low-wavelength light scattered from them, and, when looking through them towards a white light source, they appear transparent with a reddish tinge since the blue light is preferentially scattered away. The relative transparency of nanoemulsions makes them ideal candidates for probe-based optical studies, such as microrheology. However, as the droplet radius approaches 100 nm, nanoemulsions appear hazy, and above this, in the submicron range, they appear white due to significant multiple scattering. Thus, one easy way

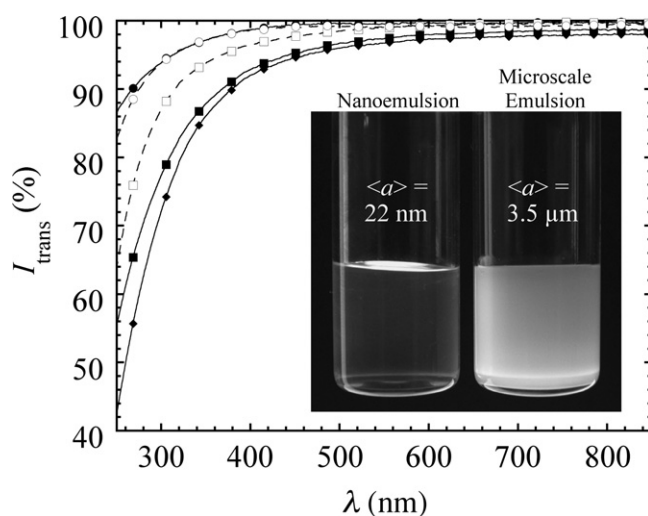


**Figure 12.** Ultraviolet–visible spectroscopy of nanoemulsions having  $\langle a \rangle = 40$  nm in a 0.2 mm thick cell provides the transmitted intensity,  $I_{\text{trans}}$ , (in %) as a function of wavelength,  $\lambda$ , for a series of volume fractions:  $\phi = 0.01$  (●), 0.05 (■), 0.10 (◆), 0.25 (□), 0.45 (○). The high  $I_{\text{trans}}$  over the visible wavelength range indicates that the nanoemulsions are nearly transparent, yet they scatter significantly in the UV. Inset: 1 cm diameter glass vials contain a nanoemulsion having  $a = 22$  nm and  $\phi \approx 0.27$  (left) that is nearly transparent in the visible spectrum, and a microscale emulsion having  $a = 3.5$   $\mu\text{m}$  and  $\phi \approx 0.4$  (right) that appears white and opaque due to multiple scattering of visible light.

of telling if a nanoemulsion is coarsening by coalescence or Ostwald ripening is to simply examine its transmission as a function of time at a fixed wavelength in the visible range. Optical transparency is also a good qualitative indicator of significant polydispersity since any extension of the tail of the size distribution toward microscale droplet sizes will make the nanoemulsion appear hazy, even if the vast majority of the droplets are truly nanoscale.

Some mechanical shear or ‘rheological’ properties of nanoemulsions are also affected by the nanoscale size of the droplets. As with microscale emulsions, the rheological properties depend strongly on whether the droplets interact repulsively or attractively [21, 17]. For very dilute  $\phi$ , the shear viscosity of repulsive nanoemulsions resembles that of microscale emulsions or even hard spheres. This is because the Einstein relationship for the viscosity of a dilute dispersion of hard spheres depends only on  $\eta_c$  and  $\phi$  [4]:  $\eta(\phi) = \eta_c(1 + 5\phi/2 + \dots)$ . By contrast, at very high  $\phi$  where the droplets begin to deform, the elastic shear modulus,  $G'$ , of repulsive emulsions of all sizes is proportional to the Laplace pressure of the undeformed droplets. This implies that nanoemulsions could have exceedingly large elastic moduli, potentially approaching 1 MPa, provided that  $\Pi_d$  is not exceeded while concentrating the droplets. Although no reports exist of liquid emulsions or foams (comprised of simple Newtonian fluids) that have such large moduli, it is conceivable that they could be created. In the cases where attractive interactions between droplets become important, the droplets can form elastic yet fragile space-filling gels at volume fractions far below  $\phi_{\text{MRJ}}$ . The rheology of attractive nanoemulsion systems is only now being explored, so little information is available compared to that of microscopic emulsions. Thus, we focus on repulsive nanoemulsions for the remaining discussion.

As an example of the mechanical response of a nanoemulsion, we show the evolution of the viscoelastic storage modulus,  $G'(\omega)$ , for a repulsive, disordered nanoemulsion glass having

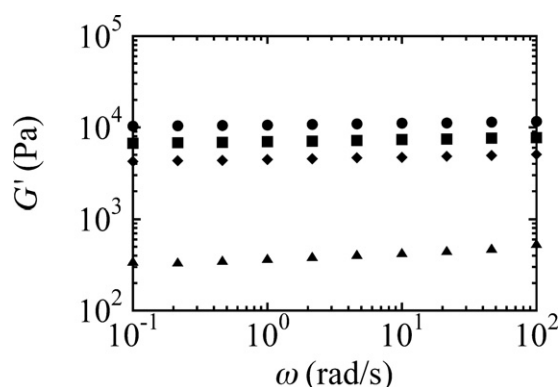


**Figure 13.** Shear elastic (storage) modulus,  $G'$ , as a function of frequency,  $\omega$ , resulting from mechanical oscillatory rheometry at a strain of 0.01 of concentrated nanoemulsions having  $\phi = 0.5$ ,  $C = 116$  mM,  $\eta_d = 10$  cP, and  $p = 90$  psi. As the emulsification proceeds, the elastic modulus of the nanoemulsion increases with pass number  $N = 1, 2, 3$ , and  $4$  (from bottom to top) as the droplet size becomes smaller. The storage modulus of the original microscale premix emulsion ( $N = 0$ ) is so low that it cannot be measured.

$\phi = 0.5$  after passing the emulsion  $N$  times through the extreme microfluidic shear device (figure 13). After each pass, a portion of the emulsion is transferred to a controlled strain rheometer. The modulus is measured at very small perturbative shear strains of about  $10^{-2}$ , so the quenched disordered droplet structure is not disturbed. The plateau in the storage modulus increases from a value that is so low that it cannot be measured for the premix emulsion ( $N = 0$ ) to well above  $10^2$  Pa after only one pass ( $N = 1$ ). Only a few more passes are required to raise the plateau modulus to  $10^4$  Pa at  $N = 4$ . This increase does not continue at the same rate, however, and the storage modulus does not grow much more even after a large number of passes. This effect of shear history on the storage modulus has not been observed for microscale emulsions at such low  $\phi$ , although it has at larger  $\phi$  [33]. This serves to illustrate a significant difference between the rheological properties of nanoscale emulsions compared to those of microscale emulsions.

Likewise, nanoemulsions exhibit enhanced shelf stability against gravitationally driven creaming over microscale emulsions at the same  $\phi$ . Brownian motion, caused by entropic driving forces, keeps the droplets suspended even over very long periods of time. The self-diffusion coefficient,  $D = k_B T / (6\pi\eta_c a)$ , where  $k_B$  is Boltzmann's constant, for oil droplets in water-based nanoemulsions is  $D \approx 10^{-8}$  to  $10^{-7}$   $\text{cm}^2 \text{s}^{-1}$  for droplets with  $a = 100$  to  $10$  nm, respectively. The gravitational height,  $h$ , associated with the colloidal law of atmospheres [4] in nanoemulsions is given by equating the gravitational potential energy of a droplet at height  $h$  above a surface with thermal energy:  $mgh = k_B T$ , where the effective buoyant mass of a droplet is  $m = 4\pi a^3 \Delta\rho / 3$ . For  $a = 10$  nm,  $\Delta\rho = 0.05$   $\text{g cm}^{-3}$ ,  $g = 980$   $\text{cm s}^{-2}$ , and  $T = 298$  K, the gravitational height is  $h = k_B T / (mg) \approx 200$  cm, well over a metre. Thus, the volume fraction of typical nanoemulsions of repulsive droplets will remain homogeneous indefinitely, even if stored in very tall containers. By contrast, repulsive microscale emulsions have  $h \approx 1$  cm, so these droplets will cream and  $\phi$  will become inhomogeneous if the emulsion is stored for a long time. If interactions between nanodroplets are changed from repulsive to significantly attractive and if  $\Delta\rho \neq 0$ , the larger aggregated flocs or clusters can cream much more rapidly than individual droplets, leading to inhomogeneous  $\phi$ . Thus, strongly attractive nanoemulsions cream as readily as strongly attractive microscale emulsions.

We have covered some of the most interesting and useful physical properties of nanoemulsions that distinguish them from their microscale counterparts. Concentrated nanoemulsions are a surprisingly transparent and elastic form of nanoscale ‘mayonnaise’. By contrast, common mayonnaise comprised of microscale droplets is commonly known to be white and a relatively soft solid. Repulsive nanoemulsions do not cream or settle much at all under earth’s gravity since entropic driving forces keep them suspended indefinitely.

## 6. Nanoemulsion science: frontiers and applications

Many exciting possibilities exist for new scientific directions and applications in the emerging field of nanoemulsions. The scientific directions include the fundamental structure and physical properties of dispersions, foams, and aggregates. Applications include personal care products, food products, and pharmaceuticals.

Understanding the structure of random monodisperse foam over a wide range of  $\phi$  between the glass transition volume fraction and the ‘dry foam-like’ limit near unity is still an open problem. Kelvin devised a structure for the minimal surface of a highly deformed droplet that packs in an ordered lattice with its neighbours in the dry limit. Although it was thought that this structure had the minimal surface area, Weaire and Phelan have shown later that, by properly packing deformed droplets having two different shapes, one can obtain a slightly lower surface area [91]. More recently, a simulation of random monodisperse foam in the dry limit has provided many important details about the distributions of edge lengths and facet sizes in random disordered foam containing bubbles that have identical volumes [57, 55, 56]. Since multiple scattering of light makes experiments on microscale and larger bubbles and droplets problematic, neutron scattering from nanoemulsions can be easily brought into the single scattering regime and is one promising method to probe this interesting structural transition. More work is clearly needed to completely understand the structure of interfaces of deformable monodisperse objects over a wide range of  $\phi$ ; monodisperse nanoemulsions may play an important role in this exploration.

Another interesting area for discovery is addressing the following simple question of emulsification: ‘How small can nanoemulsion droplets be made through extreme shear rupturing?’ Certainly, making them smaller than the physical limit of a surfactant micelle would not be realistic, but is it possible to create nanoemulsions having radii of 4 or 5 nm in which only a hundred or fewer molecules of the dispersed phase are present? The Laplace pressures would be enormous, and it is not clear how the discrete nature of higher molecular weight molecules might affect the droplet’s shape. Creating such nanoemulsions would be extremely challenging, since the shear rates required would approach  $10^{10} \text{ s}^{-1}$  for water-based systems. Moreover, treating the dispersed phase as a homogeneous liquid during the capillary instability may not be a good approximation at such length scales. Putting a rheological additive, such as a polymer, in the continuous phase in order to raise  $\eta_c$  substantially prior to exerting extreme shear may be a viable method for obtaining large quantities of nanoemulsions that have average droplet sizes below 10 nm. Thus, the whole area of emulsification in which composition and shear can be used to select a desired size and polydispersity of nanodroplets remains wide open.

The extreme Laplace pressures in nanoemulsions would facilitate fundamental studies of Ostwald ripening by reducing the total time for an experiment due to the faster coarsening rates. In silicone oil-in-water nanoemulsions, the solubility of the oil molecules in the water phase is strongly dependent on the molecular weight,  $M_w$ , (i.e. length) of the siloxane polymer chains. Assuming that the energy cost per unit of molecular weight of the polymer to be surrounded by water molecules is  $\varepsilon$ , the equilibrium probability of having the molecules in solution would be proportional to the Boltzmann factor,  $\exp[-\varepsilon M_w / (k_B T)]$ , assuming that the

polymers cannot collapse on themselves. Thus, the probability becomes exponentially smaller for longer polymers, thereby reducing the rate of Ostwald ripening. Since more viscous oils have higher molecular weights, typically Ostwald ripening is not observed for  $\eta_d > 10$  cP, even for droplets approaching 10 nm in radius. However, for  $\eta_d \approx 1$  cP, the polymer chains are so short that they can have significant solubility in the aqueous continuous phase. Since the Laplace pressure of the droplets is so large, at reasonably high  $\phi > 0.1$ , the diffusively driven coarsening can become very rapid. In this case, the nanoemulsion destabilizes quickly, and, immediately after emulsification, its optical properties change spontaneously from translucent to white as the droplets coarsen into microscale and larger droplets through Ostwald ripening.

The compositional flexibility of nanoemulsions offers a wide range of applications. The incorporation of fluorescent dyes and other molecules into nanoemulsions makes them interesting probes for exploring properties of living cells and for drug delivery. The deformable and liquid nature of the droplets may lead to discoveries of new pathways for cellular uptake and dispersal. Both oil-soluble and water-soluble drug molecules can be incorporated into the nanodroplets of direct and inverse nanoemulsions for potential pharmaceutical uses.

In the personal care and food industries, nanoemulsions may provide interesting alternatives as pleasantly transparent and soft solids that possess plastic-like rheological properties. While being appealing from an optical and rheological point of view, nanoemulsions also can deliver moisturizers to the skin quite efficiently and also block ultraviolet light without leaving a white residue. The small size of the nanodroplets will likely increase transport efficiency of any active drugs or other molecules inside the droplets across biological membranes, including the skin. Thus, nanoemulsions may have significant applications in medical patches.

In the printing and data storage industries, one may imagine the resolution of using zeptolitre droplets instead of picolitre droplets. The precise manipulation and deposition of such tiny droplets pose many technological hurdles, but the potential exists for creating piezo-driven and thermally-driven printers using nanoemulsion inks.

The few examples covered in this section only begin to scratch the surface of the many potential scientific discoveries and applications that will arise from nanoemulsion research. High-throughput production methodologies make nanoemulsions a realistic commercial-scale alternative for diverse areas, including lotions and pharmaceuticals. Nanoemulsions represent a very flexible platform for producing soft materials that can be tailored in their composition and also in their optical, rheological, and stability properties. Through fractionation, they can also be made into model materials that can provide important scientific insights into the basic structure of disordered glasses and attractive gels. Overall, nanoemulsions represent an intriguing new class of dispersions that may someday rival or surpass their microscale counterparts in commercial importance.

## 7. Conclusion

This review has captured much of the current activity surrounding the formation, physical properties, and structure of nanoemulsions, and it has provided motivation for more research and applications. Just as colloidal dispersions of solid nanoscale particulates have received considerable attention, colloidal dispersions of deformable nanodroplets—'nanoemulsions'—are beginning to receive significant attention. Although many basic principles of emulsification are already known for isolated droplets in relatively mild shear flows, the new principles of emulsification that govern nanodroplet rupturing and coalescence in extreme shear at high  $\phi$  are still being discovered. Quantitative theoretical predictions of droplet size distributions that include the combination of these two effects are sorely needed. Once formed, nanoemulsions

can be manipulated and controlled in very precise ways. Ultracentrifugal fractionation provides model monodisperse dispersions of nanoscale droplets in the size range from roughly  $a = 10$  to 100 nm. These monodisperse nanoemulsions have proven to be very useful in combination with neutron scattering methods to reveal the average bulk positional structures as droplet interactions range from repulsive to strongly attractive. Through rapid osmotic compression, dilute nanoemulsions of repulsive droplets can be transformed into transparent soft elastic solids that can have surprisingly strong shear elasticity. Such materials have many potential scientific applications, such as exploring size-dependent droplet uptake through the membranes of living cells. Moreover, the development of high-throughput production makes the potential for widespread commercial use of nanoemulsions in consumer products and medical applications highly likely. In the future, we predict that nanoemulsions will become as ubiquitous as many polymer solutions and solid particulate dispersions are today.

### Acknowledgments

We thank Dr John McTague for generously supporting this work. We have enjoyed helpful discussions with Dr Charles Knobler, Dr Robijn Bruinsma, Dr Andrew Kraynik, Dr Alex Levine, and Dr Sascha Hilgenfeldt. The author thanks APS, ACS, and Taylor and Francis for permission to reproduce figures. Material from Taylor and Francis is copyright 2004 from Soft Materials by T G Mason. Reproduced by permission of Taylor and Francis Group, LLC., <http://www.taylorandfrancis.com>.

### References

- [1] Meleson K, Graves S and Mason T G 2004 Formation of concentrated nanoemulsions by extreme shear *Soft Mater.* **2** 109
- [2] Landfester K, Tiarks F, Hentze H and Antonietti M 2000 Polyaddition in miniemulsions: a new route to polymer dispersions *Macromol. Chem. Phys.* **201** 1
- [3] Walstra P 1996 *Encyclopedia of Emulsion Technology* vol 4, ed P Becher (New York: Dekker) p 1
- [4] Russel W B, Saville D A and Schowalter W R 1989 *Colloidal Dispersions* (Cambridge: Cambridge University Press)
- [5] Solans C, Izquierdo P, Nolla J, Azemar N and Garcia-Celma M J 2005 Nano-emulsions *Curr. Opin. Colloid Interface Sci.* **10** 102
- [6] Bibette J, Roux D and Nallet F 1990 Depletion interactions and fluid–solid equilibrium in emulsions *Phys. Rev. Lett.* **65** 2470
- [7] Dimon P, Sinha S K, Weitz D A, Safinya C R, Smith G S, Varady W A and Lindsay H M 1986 Structure of aggregated gold colloids *Phys. Rev. Lett.* **57** 595
- [8] Lin M Y, Lindsay H M, Weitz D A, Klein R, Ball R C and Meakin P 1990 Universal diffusion-limited colloid aggregation *J. Phys.: Condens. Matter* **2** 3093
- [9] Becher P 1965 *Emulsions: Theory and Practice* (New York: Reinhold)
- [10] Bibette J, Leal-Calderon F and Poulin P 1999 Emulsions: Basic principles *Rep. Prog. Phys.* **62** 969
- [11] Myers D 1999 *Surfaces, Interfaces, and Colloids* (New York: Wiley)
- [12] Diat O, Roux D and Nallet F 1993 Effect of shear on a lyotropic lamellar phase *J. Physique II* **3** 1427
- [13] Bibette J, Morse D C, Witten T A and Weitz D A 1992 Stability criteria for emulsions *Phys. Rev. Lett.* **69** 2439
- [14] Taylor P 2003 Ostwald ripening in emulsions: Estimation of solution thermodynamics of the disperse phase *Adv. Colloid Interface Sci.* **106** 261
- [15] Durian D J, Weitz D A and Pine D J 1991 Multiple light-scattering probes of foam structure and dynamics *Science* **252** 686
- [16] Gopal A D and Durian D J 2003 Relaxing in foam *Phys. Rev. Lett.* **91** 188303
- [17] Mason T G, Krall A H, Gang H, Bibette J and Weitz D A 1996 *Encyclopedia of Emulsion Technology* vol 4, ed P Becher (New York: Dekker) p 299
- [18] Taylor G I 1934 The formation of emulsions in definable fields of flow *Proc. R. Soc. A* **146** 501
- [19] Hinch E J and Acrivos A 1980 Long slender drops in a simple shear flow *J. Fluid Mech.* **98** 305

- [20] Rallison J M 1984 The deformation of small viscous drops and bubbles in shear flows *Annu. Rev. Fluid Mech.* **16** 45
- [21] Mason T G 1999 New fundamental concepts in emulsion rheology *Curr. Opin. Colloid Interface Sci.* **4** 231
- [22] Chandrasekhar S 1961 *Hydrodynamic and Hydromagnetic Stability* (London: Oxford University Press)
- [23] Mikami T, Cox R G and Mason S G 1975 Breakup of extending liquid threads *Int. J. Multiph. Flow* **2** 113
- [24] Renardy Y Y and Cristini V 2001 Scalings for fragments produced from drop breakup in shear flow with inertia *Phys. Fluids* **13** 2161
- [25] Kim Y-H, Koczo K and Wasan D T 1997 Dynamic film and interfacial tensions in emulsion and foam systems *J. Colloid Interface Sci.* **187** 29
- [26] Khakhar D V and Ottino J M 1987 Breakup of liquid threads in linear flows *Int. J. Multiph. Flow* **13** 71
- [27] Eggleton C D, Tsai T-M and Stebe K J 2001 Tip streaming from a drop in the presence of surfactants *Phys. Rev. Lett.* **87** 048302
- [28] Anna S L, Bontoux N and Stone H A 2003 Formation of dispersions using flow focusing in microchannels *Appl. Phys. Lett.* **82** 364
- [29] Renardy Y Y and Cristini V 2001 Effect of inertia on drop breakup under shear *Phys. Fluids* **13** 7
- [30] Mason T G, Bibette J and Weitz D A 1996 Yielding and flow of monodisperse emulsions *J. Colloid Interface Sci.* **179** 439
- [31] Mason T G and Bibette J 1996 Emulsification in viscoelastic media *Phys. Rev. Lett.* **77** 3481
- [32] Mason T G and Bibette J 1997 Shear rupturing of droplets in complex fluids *Langmuir* **13** 4600
- [33] Mason T G and Rai P K 2003 Shear-induced elastification of concentrated emulsions probed by sinusoidal amplitude variation rheometry *J. Rheol.* **47** 513
- [34] Migler K B 2001 String formation in sheared polymer blends: Coalescence, breakup, and finite size effects *Phys. Rev. Lett.* **86** 1023
- [35] Mason T G, Lacasse M-D, Grest G S, Levine D, Bibette J and Weitz D A 1997 Osmotic pressure and viscoelastic shear moduli of concentrated emulsions *Phys. Rev. E* **56** 3150
- [36] Raff L M 2001 *Principles of Physical Chemistry* (Upper Saddle River, NJ: Prentice-Hall)
- [37] Pusey P N and van Meegen W 1986 Phase behaviour of concentrated suspensions of nearly hard colloidal spheres *Nature* **320** 340
- [38] Reinelt D A and Kraynik A M 1996 Simple shearing flow of a dry Kelvin soap foam *J. Fluid Mech.* **311** 327
- [39] Stamenovic D 1991 A model of foam elasticity based upon the laws of plateau *J. Colloid Interface Sci.* **145** 255
- [40] Kraynik A M and Reinelt D A 1996 Linear elastic behavior of dry soap foams *J. Colloid Interface Sci.* **181** 511
- [41] Stone H A, Koehler S A, Hilgenfeldt S and Durand M 2003 Perspectives on foam drainage and the influence of interfacial rheology *J. Phys.: Condens. Matter* **15** S283
- [42] Lacasse M-D, Grest G S, Levine D, Mason T G and Weitz D A 1996 A model for the elasticity of compressed emulsions *Phys. Rev. Lett.* **76** 3448
- [43] Liu A J and Nagel S R 1998 Jamming is not just cool any more *Nature* **396** 21
- [44] O'Hern C S, Langer S A, Liu A J and Nagel S R 2002 Random packings of frictionless particles *Phys. Rev. Lett.* **88** 075507
- [45] Pusey P N and van Meegen W 1987 Observation of a glass transition in suspensions of spherical colloidal particles *Phys. Rev. Lett.* **59** 2083
- [46] van Meegen W and Underwood S M 1994 Glass transition in colloidal hard spheres: Measurement and mode-coupling-theory analysis of the coherent intermediate scattering function *Phys. Rev. E* **49** 4206
- [47] Mason T G and Weitz D A 1995 Linear viscoelasticity of colloidal hard sphere suspensions near the glass transition *Phys. Rev. Lett.* **75** 2770
- [48] Mason T G, Bibette J and Weitz D A 1995 Elasticity of compressed emulsions *Phys. Rev. Lett.* **75** 2051
- [49] Lacasse M-D, Grest G S and Levine D 1996 Deformation of small compressed droplets *Phys. Rev. E* **54** 5436
- [50] Mason T G, Gang H and Weitz D A 1997 Optical measurements of the linear viscoelastic moduli of complex fluids *J. Opt. Soc. Am. A* **14** 139
- [51] Torquato S, Truskett T M and Debenedetti P G 2000 Is random close packing of spheres well defined? *Phys. Rev. Lett.* **84** 2064
- [52] Bernal J D and Mason J 1960 Coordination of randomly packed spheres *Nature* **188** 910
- [53] Beryman J G 1983 Random close packing of hard spheres and disks *Phys. Rev. A* **27** 1053
- [54] Donev A, Cisse I, Sachs D, Variano E A, Stillinger F H, Connelly R, Torquato S and Chaikin P M 2003 Improving the density of jammed disordered packings using ellipsoids *Science* **303** 990
- [55] Kraynik A M, Reinelt D A and van Swol F 2003 Structure of random monodisperse foam *Phys. Rev. E* **67** 031403
- [56] Kraynik A M 2003 Foam structure: From soap froth to solid foams *MRS Bull.* **28** 275
- [57] Kraynik A M, Reinelt D A and van Swol F 2004 Structure of random foam *Phys. Rev. Lett.* **93** 208301
- [58] Bibette J, Mason T G, Gang H, Weitz D A and Poulin P 1993 Structure of adhesive emulsions *Langmuir* **9** 3352

- [59] Philip J, Bonakdar L, Poulin P, Bibette J and Leal-Calderon F 2000 Viscous sintering phenomena in liquid–liquid dispersions *Phys. Rev. Lett.* **84** 2018
- [60] Reiss H 1975 Entropy-induced dispersion of bulk liquids *J. Colloid Interface Sci.* **53** 61
- [61] Miller C A 2006 *Emulsions and Emulsion Stability* ed J Sjoblom (Boca Raton, FL: Taylor and Francis) p 107
- [62] Whitesides G M and Grzybowski B 2002 Self-assembly at all scales *Science* **295** 2418
- [63] Tlusty T and Safran S A 2000 Microemulsion networks: The onset of bicontinuity *J. Phys.: Condens. Matter* **12** A253
- [64] Weaire D, Hutzler S, Cox S, Kern N, Alonso M D and Drenckham W 2003 The fluid dynamics of foam *J. Phys.: Condens. Matter* **15** S65
- [65] Hilgenfeldt S, Kraynik A M, Koehler S A and Stone H A 2001 An accurate von Neumann's law for three-dimensional foams *Phys. Rev. Lett.* **86** 2685
- [66] Hansen F K and Ugelstad J 1979 Particle nucleation in emulsion polymerization: 4. Nucleation in monomer droplets *J. Polym. Sci. A* **17** 3069
- [67] Choi Y T, El-Aasser M S, Sudol E D and Vanderhoff J W 1985 Polymerization of styrene miniemulsions *J. Polym. Sci. A* **23** 2973
- [68] Tang P L, Sudol E D, Silebi C A and El-Aasser M S 1991 Miniemulsion polymerization—a comparative-study of preparative variables *J. Appl. Polym. Sci.* **43** 1059
- [69] Sudol E D and El-Aasser M S 1997 *Emulsion Polymerization and Emulsion Polymers* ed P A Lovell and M S El-Aasser (Chichester: Wiley)
- [70] Johnson C S and Gabriel D A 1981 *Laser Light Scattering* (New York: Dover)
- [71] Roe R-J 2000 *Methods of X-ray and Neutron Scattering in Polymer Science* (Oxford: Oxford University Press)
- [72] Slayter E M and Slayter H S 1992 *Light and Electron Microscopy* (New York: Cambridge)
- [73] Webster A J and Cates M E 2001 Osmotic stabilization of concentrated emulsions and foams *Langmuir* **17** 595
- [74] Bird R B, Armstrong R C and Hassager O 1977 *Dynamics of Polymeric Liquids* vol I (New York: Wiley)
- [75] Ferry J D 1980 *Viscoelastic Properties of Polymers* (New York: Wiley)
- [76] Squires T M and Quake S R 2005 Microfluidics: Fluid physics at the nanoliter scale *Rev. Mod. Phys.* **77** 977
- [77] Leal L G 2004 Flow induced coalescence of drops in a viscous liquid *Phys. Fluids* **16** 1833
- [78] Mason T G, Graves S M, Wilking J N and Lin M Y 2006 Extreme emulsification: Formation and structure of nanoemulsions *Condens. Matter Phys.* **9** 193
- [79] Asakura S and Oosawa F 1954 On interaction between two bodies immersed in a solution of macromolecules *J. Chem. Phys.* **22** 1255
- [80] Bibette J 1991 Depletion interactions and fractionated crystallization for polydisperse emulsion purification *J. Colloid Interface Sci.* **147** 474
- [81] Schaffinger U 1990 Centrifugal separation of a mixture *Fluid Dyn. Res.* **6** 213
- [82] Graves A, Meleson K, Wilking J, Lin M Y and Mason T G 2005 Structure of concentrated nanoemulsions *J. Chem. Phys.* **122** 134703
- [83] Mason T G, Graves S M, Wilking J N and Lin M Y 2006 Effective structure factor of osmotically deformed nanoemulsions *J. Phys. Chem.* doi:10.1021/jp0601623
- [84] Wilking J N, Graves S N, Chang C B, Meleson K, Lin M Y and Mason T G 2006 Dense cluster formation during aggregation and gelation of attractive slippery nanoemulsion droplets *Phys. Rev. Lett.* **96** 015501
- [85] Hansen J-P and McDonald I R 1990 *Theory of Simple Liquids* (London: Academic)
- [86] Ashcroft N W and Lekner J 1966 Structure and resistivity of liquid metals *Phys. Rev.* **145** 83
- [87] Baxter R J 1968 Ornstein–Zernike relation for a disordered fluid *Aust. J. Phys.* **21** 563
- [88] Chaikin P M and Lubensky T 1995 *Principles of Condensed Matter Physics* (Cambridge: Cambridge University Press)
- [89] Witten T A and Sander L M 1981 Diffusion-limited aggregation: A kinetic critical phenomenon *Phys. Rev. Lett.* **47** 1400
- [90] van de Hulst H C 1981 *Light Scattering by Small Particles* (New York: Dover)
- [91] Weaire D and Phelan R 1994 A counter-example to Kelvin's conjecture on minimal surfaces *Phil. Mag. Lett.* **69** 107